ACS OMEGA

Open Access

http://pubs.acs.org/journal/acsodf

Article

TMEM147: A Promising Cancer Biomarker Associated with Immune Cell Infiltration and Prognosis in LIHC—Insights from a Comprehensive Pan-Cancer Genomic Analysis

Yongqing Li, Hanxiang Chen, Bingyang Zhang, Junjun Liu, Jianping Ma, Wanshan Ma, and Sumei Lu*

Cite This: *ACS Omega* 2024, 9, 27137−27157

Read Online

ACCESS | Metrics & More | Article Recommendations

ABSTRACT: Previous studies have demonstrated the regulatory roles of Transmembrane protein 147 (TMEM147) in various diseases, including cancer. However, systematic pan-cancer analyses investigating the role of TMEM147 in diagnosis, prognosis, and immunological prediction are lacking. An analysis of data from The Cancer Genome Atlas (TCGA) revealed differential TMEM147 expression across various types of cancer as well as within immune and molecular cancer subtypes. Moreover, high TMEM147 expression was associated with poor disease-specific survival (DSS), overall survival (OS), and progression-free interval (PFI) across cancers, suggesting its potential as a prognostic biomarker. Our study further revealed a significant correlation between TMEM147 expression and T helper cell and Tcm cell infiltration in most cancer types. In the case of liver hepatocellular carcinoma (LIHC), the effect of TMEM147 on prognosis varied among different clinical subtypes. Additionally, functional enrichment analysis revealed an association between TMEM147 and metabolic pathways. Finally, experiments on the MIHA cell line and four LIHC cell lines confirmed the role of TMEM147 in promoting liver cancer cell proliferation, further confirming the clinical value of TMEM147 in liver cancer diagnosis. Our findings suggest that TMEM147 may serve as a diagnostic and prognostic biomarker across cancers while also playing a significant role in LIHC.

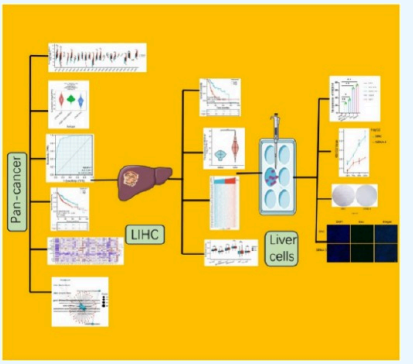

INTRODUCTION

Membrane proteins account for a significant proportion of total cellular proteins; these proteins are anchored to cell membranes and play crucial roles in regulating intercellular interactions and cellular interactions with the surrounding environment. Due to their inter- and intracellular biological signaling functions, numerous membrane proteins have been implicated in cancer development, cancer cell metastasis, and immune-related disorders.[1] These poorly characterized transmembrane proteins belong to the Transmembrane protein (TMEM) family, which includes a diverse range of transmembrane proteins that are found in various cellular membranes, such as endoplasmic reticulum (ER), mitochondrial, and lysosomal membranes. TMEM proteins are involved in many biological processes,[2] and TMEM proteins have been demonstrated to be involved in tumor metastasis. For instance, TMEM48 contributes to the invasive metastasis of lung cancer cells,[3] while TMEM206 enhances the metastasis and invasion of colon cancer cells by activating the AKT and FAK pathways.[4] Additionally, TMEM176 expression has been shown to be increased in lymphoma, breast cancer, liver cancer, and other malignancies compared to normal tissues.[5] These findings collectively indicate that TMEM proteins are promising potential biomarkers and prognostic indicators in cancer.

TMEM147, which is a member of the TMEM family, is a transmembrane protein that includes seven transmembrane domains. TMEM147 has a molecular mass of 25 kDa and predominantly localizes to the ER membrane and the nuclear envelope. Moreover, TMEM147 is an integral component of the nicalin-TMEM147-NOMO protein complex.[6,7] Based on published studies, dysregulation of TMEM147 expression may contribute to the pathogenesis of various diseases via diverse mechanisms. A clinical study demonstrated that TMEM147 deficiency leads to the upregulation of CKAP4 (CLIMP-63) and RTN4 (NOGO), accompanied by ER redirection. Children with TMEM147 deficiency present consistent clinical features, such as coarse facial features, developmental delays, intellectual disability, and behavioral problems. These findings suggest that biallelic loss-of-function TMEM147 variants cause syndromic intellectual disability, ER translocations, and nuclear tissue dysfunction.[6] TMEM147 is a membrane receptor that interacts with galactose lectin, thereby influencing both host innate

Received: February 6, 2024
Revised: May 9, 2024
Accepted: June 4, 2024
Published: June 11, 2024

immune responses and parasite immune responses by regulating cellular proliferation and phagocytosis. Additionally, TMEM147 mediates the transcription and production of nitric oxide, transforming growth factor β1 (TGF-β1), and interleukin 10 (IL-10).[8] Furthermore, knockdown of TMEM147 substantially decreases the abundance of the nuclear envelope protein lamin B receptor (LBR) and causes its mislocalization within the ER. Additionally, TMEM147 physically interacts with DHCR7, which is an enzyme that is crucial for cholesterol biosynthesis; thus, TMEM147 is an important novel regulator of intracellular cholesterol homeostasis.[9] Moreover, TMEM147 is a major activator of NF-κB in chondrocytes and is expressed at elevated levels in chondrocytes from individuals with rheumatoid arthritis (RA); these findings suggest its involvement in the pathogenesis of RA.[10] Furthermore, TMEM147 exhibits differential expression patterns in colon cancer and osteosarcoma, making it a potential tumor biomarker.[2,11] Despite reports on the role of TMEM147 in diverse physiopathological processes, the functional characteristics of TMEM147 remain poorly understood; in particular, systemic analyses across cancers are lacking.

By integrating data from The Cancer Genome Atlas (TCGA) and the Gene Expression Omnibus (GEO) databases, our recent study revealed differential expression of TMEM147 in more than 20 distinct types of cancer. This differential expression was evident even among various molecular or immune subtypes within the same type of cancer, suggesting that TMEM147 may serve as a pan-cancer biomarker. Furthermore, analyses of the associations between TMEM147 expression and overall survival (OS), disease-specific survival (DSS), and progression-free interval (PFI) revealed that elevated TMEM147 expression is associated with unfavorable prognosis. Moreover, Kyoto Encyclopedia of Genes and Genomes (KEGG), Gene Ontology (GO), and GSEA analyses were performed to determine shared biological pathways and to conduct enrichment analysis of the differentially expressed genes. Subsequently, we focused on liver hepatocellular carcinoma (LIHC) and revealed correlations between TMEM147 expression and various clinical characteristics. Finally, experiments on liver cell lines were conducted to confirm the role of TMEM147 in liver cancer. The current investigation of the role of TMEM147 across cancers will undoubtedly provide additional evidence to facilitate subsequent clinical translation.

MATERIALS AND METHODS

Data Preprocessing and Gene Expression Analysis. Transcriptional RNA sequencing (RNA-Seq) expression profiles and the corresponding clinical information for 33 types of cancer were obtained from the TCGA database sharing data portal (https://portal.gdc.cancer.gov/) and the Genotype-Tissue Expression (GTEx) database (https://commonfund.nih.gov/GTEx) from UCSC Xena (https://xenabrowser.net/datapages/). The data were transformed to transcripts per kilobase million (TPM) via the Toil process.[12] R software v3.6.3 was used for statistical analysis, and the ggplot2 package was used for visualization. The Wilcoxon signed rank test was used to analyze differences among all the transcriptomic data, and $P < 0.05$ was considered to indicate statistical significance (ns, $P \geq 0.05$; *$P < 0.05$; **$P < 0.01$; ***$P < 0.001$).

Diagnostic Value Analysis. Receiver operating characteristic (ROC) curves were used to assess the diagnostic value of TMEM147 in 33 types of cancer, and the pROC package was used for analysis. The area under the curve (AUC) ranged from 0.5 to 1.0; 0.5−0.7 indicated low accuracy, 0.7−0.9 indicated medium accuracy, and 0.9 or higher indicated high accuracy.

Analysis of TMEM147 Expression in Different Immunological and Molecular Subtypes of Human Cancers. The TISIDB database (http://cis.hku.hk/TISIDB/index.php), which is a web portal for information on tumor and immune system interactions that integrates multiple heterogeneous data types, was used to determine the relationships between TMEM147 expression and immune or molecular subtypes across cancers. Results with a P value <0.05 were considered statistically significant, and they are shown in Results.

Interaction Network Analysis and Functional Clustering Analysis. The String (https://string-db.org/) database was used to construct a protein−protein interaction (PPI) network of TMEM147. The network was constructed by searching for the protein name of TMEM147 in *Homo sapiens* and setting the main parameters to medium confidence and active interaction sources. Cytoscape (v3.9.1) was used for visualization.

GO and KEGG enrichment analyses were conducted with the clusterProfiler package (v3.14.3), and the results were visualized with the ggplot2 package.[13] The KEGG pathways and GO_BP terms were examined using the gene set enrichment analysis (GSEA) function module.

Prognosis Analysis. The relationships between TMEM147 and OS and between DSS and the PFI were investigated using Kaplan−Meier plots. The Survminer package (v0.4.9) was used for visualization, and the survival package was used for statistical analysis of survival data.[14] All the data were obtained from the TCGA database in HTSeq-FPKM format and transformed into the TPM format.

Clinical Correlation Analysis in LIHC. Data from the TCGA-LIHC database in the level 3 HTSeq-fragments per kilobase per million (FPKM) format were downloaded from the TCGA database, converted to the transcripts per million reads (TPM) format, and then analyzed after log2 transformation. Ggplot2 (v3.3.3) was used for visualization. Different clinical characteristics related to LIHC, such as age, weight, AFP (ng/mL), and Child−Pugh score, were included.

Coexpression Analysis and Enrichment Analysis of TMEM147 in LIHC. Genes that were coexpressed with TMEM147 were identified by R based on the expression profiles of the TCGA cohort. The top 50 genes that were positively and negatively related to TMEM147 in LIHC were identified, and they are shown. Ggplot2 was used for visualization. Then, we used all of the genes that were coexpressed with TMEM147 in LIHC for enrichment analysis.

Analysis of Immune Cell Infiltration across Cancer Types and in LIHC. The markers of 24 kinds of immune cells were confirmed[15] using the ssGSEA immune infiltration algorithm and GSVA package to determine the immune profiles across cancer types and in LIHC.[16]

Cell Culture. The cell lines that were used in this study included the MIHA, BEL-7402, SMMC 7721, HepG2, and Huh-7 cell lines. MIHA cells were cultured in 1640 medium (Gibco, USA) supplemented with 10% fetal bovine serum (FBS) (Gibco, USA). The remaining cell lines were cultured in DMEM (Gibco, USA) supplemented with 10% FBS. All the cell cultures were maintained in a humidified incubator at 37 °C with 5% CO_2. Subculturing was routinely performed when the cells reached 80−90% confluence using trypsin-EDTA (Gibco, USA). Cell viability was assessed during each passage using the trypan blue exclusion assay (Gibco, USA).

https://doi.org/10.1021/acsomega.4c01215
ACS Omega 2024, 9, 27137−27157

Real-Time PCR and Western Blotting. Real-time PCR and western blotting were used to analyze gene expression. For real-time PCR, cDNA was synthesized by reverse transcription, followed by amplification with gene-specific primers. The sequences of the synthetic primers are shown in Table 1.

Table 1. Sequences of Synthetic Primers and siRNAs

gene	sequence
Homo-TMEM147	forward: 5′- CGGGGCATTGAGTTTGACTG-3′; reverse: 3′-AGACGCGACGATGTAATGGA-5′
siRNA-1	forward: 5′-CCUACUUCAUCACCUACAATT-3′; reverse: 3′- UUGUAGGUGAUGAAGUAGGTT-5′
siRNA-2	forward: 5′-GCAGACCUGAUAGGUCUAATT-3′; reverse: 3′- UUAGACCUAUCAGGUCUGCTT-5′
siRNA-3	forward: 5′- CCACUGCUGAGCUUAUUAUTT-3′; reverse: 3′- AUAAUAAGCUCAGCAGUGGTT-5′
siRNA-4	forward: 5′- GUGUCUACAAGGCCUUUGUTT-3′; reverse: 3′- ACAAAGGCCUUGUAGACACTT-5′

Western blotting analysis included protein extraction, protein separation by SDS−PAGE, protein transfer to PVDF membranes, and protein detection using primary antibodies against the proteins of interest. The utilization of these established methodologies ensured the reliable and accurate evaluation of gene expression in our study.

Cell Colony Formation Assay. HepG2 and Huh-7 cells were cultured in DMEM supplemented with 10% FBS and 1% penicillin−streptomycin. siRNAs were purchased from Biosune, and the sequences of the siRNAs are shown in Table 1. The experiment was performed in six-well plates, and 4% paraformaldehyde and a 0.1% crystal violet staining solution were used in this experiment.

Huh-7 and HepG2 cells were seeded at a density of 2×10^4 or 2×10^5 cells per well, respectively, and cultured for 16 h. The cells were then transfected with siRNAs for 24 h using Lipofectamine 2000. The cells were subsequently fixed with 4% paraformaldehyde, stained with 0.1% crystal violet, and observed under a microscope.

CCK-8 Assay. Following siRNA transfection, the cells were incubated for 24, 72, 96, or 120 h. At each time point, the culture medium was replaced with fresh DMEM supplemented with CCK-8 reagent (Cell Counting Kit-8), and the cells were incubated for an additional 2 h at 37 °C in a humidified incubator. After the incubation period, the absorbance of the formazan dye, which is directly proportional to the number of viable cells, was measured at 450 nm using a microplate reader.

EdU Assay. After 72 h of siRNA transfection, the proliferation of the cells was assessed using the Click-iT EdU Alexa Fluor 488 Imaging Kit. Briefly, the cells were labeled with EdU, which is a nucleoside analog that is incorporated into newly synthesized DNA during active DNA replication. The cells were incubated with EdU labeling medium for 2 h at 37 °C. Following incubation, the cells were fixed with 4% paraformaldehyde and permeabilized with 0.3% Triton X-100. The incorporated EdU was then detected by a Click-iT reaction with Alexa Fluor 488 dye. Nuclei were counterstained with 4′,6-diamidino-2-phenylindole (DAPI).

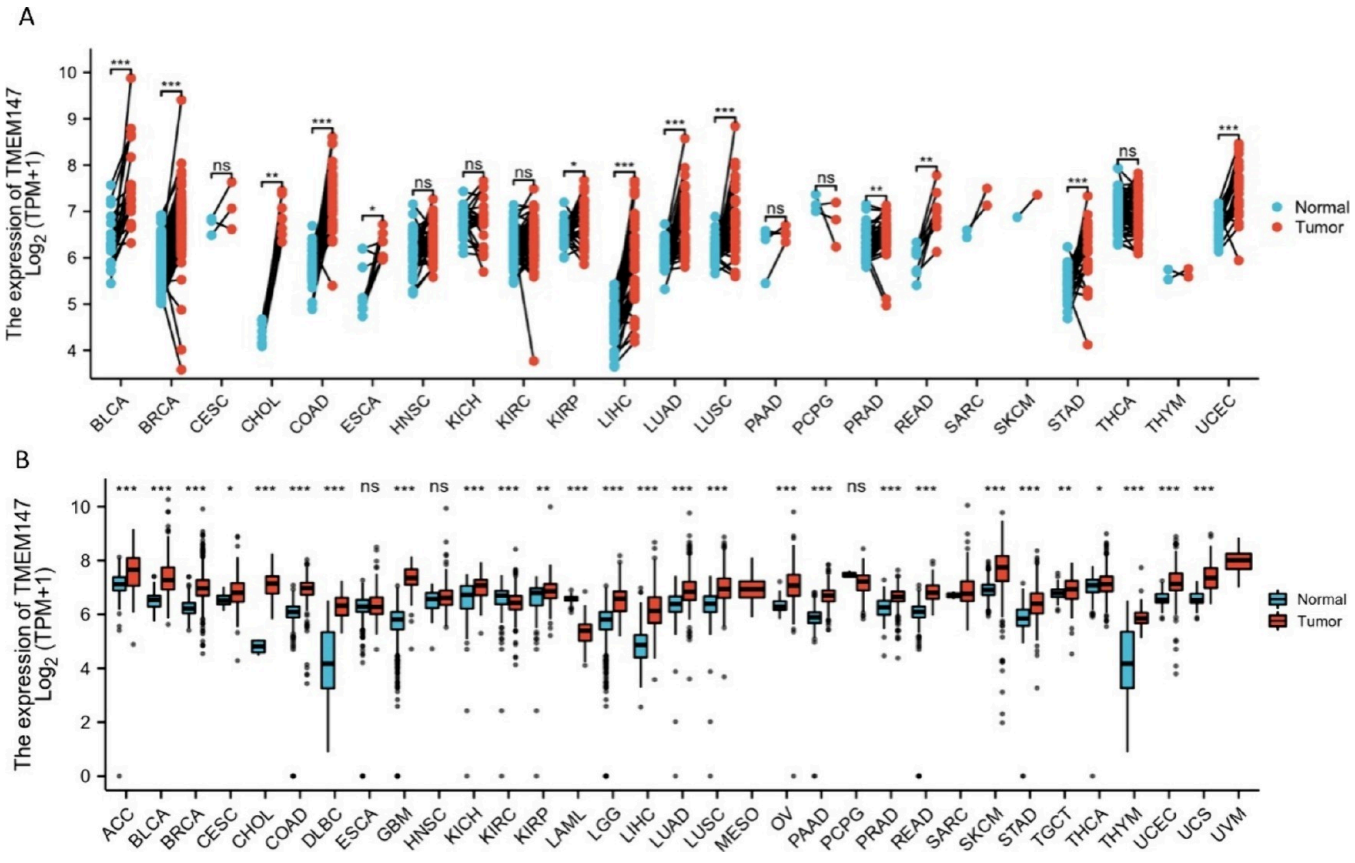

Figure 1. Expression level of the TMEM147 gene in tumor tissues and normal tissues. (A) TMEM147 expression in tumor tissues and adjacent normal tissues from the TCGA database; (B) TMEM147 expression in tumor tissues and normal tissues from the TCGA database when data from the GTEx database were used as controls (*$P < 0.05$, ** $P < 0.01$, *** $P < 0.001$).

https://doi.org/10.1021/acsomega.4c01215
ACS Omega 2024, 9, 27137−27157

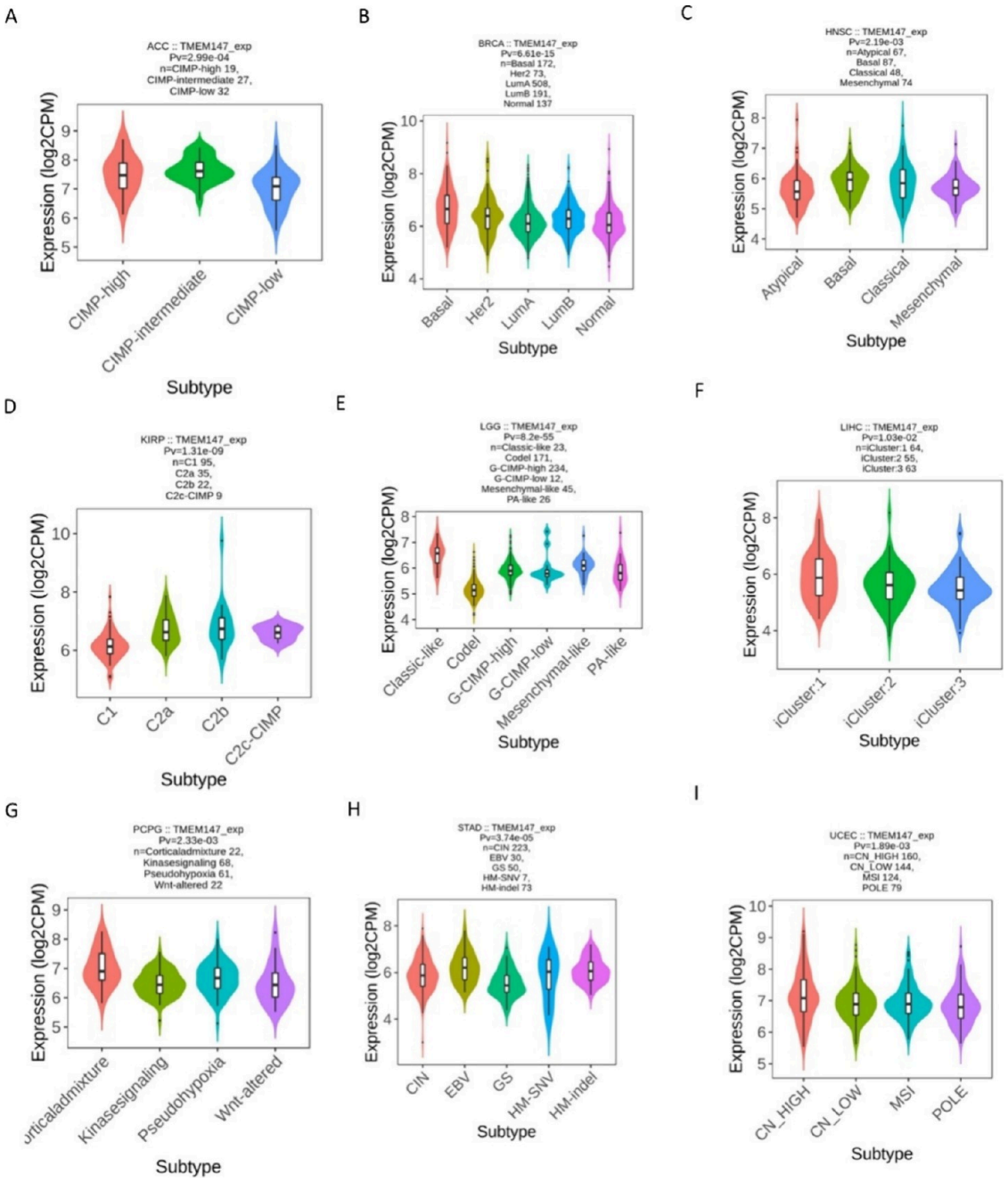

Figure 2. Correlations between TMEM147 expression and molecular subtypes across TCGA tumors. (A) ACC; (B) BRCA; (C) HNSC; (D) KIRP; (E) LGG; (F) LIHC; (G) PCPG; (H) STAD; (I) UCEC.

RESULTS

TMEM147 Expression Levels Were Increased across Various Cancer Tissues. The expression profiles of TMEM147 across many cancer types in the TCGA database were analyzed. As shown in Figure 1A, among all 18 types of cancer that were investigated, TMEM147 was significantly more highly expressed in 13 types of cancer—bladder urothelial carcinoma (BLCA), breast invasive carcinoma (BRCA), cholangiocarcinoma (CHOL), colon adenocarcinoma (COAD), esophageal carcinoma (ESCA), kidney renal papillary cell carcinoma (KIRP), liver hepatocellular carcinoma (LIHC), lung adenocarcinoma (LUAD), lung squamous cell carcinoma (LUSC), prostate adenocarcinoma (PRAD), rectal adenocarcinoma (READ), stomach adenocarcinoma (STAD), and uterine corpus endometrial carcinoma (UCEC)—than in cancer-adjacent normal tissues. Data from the GTEx database were used as controls, and TMEM147 was also found to be highly expressed in 27 out of 33 cancer types (Figure 1B).

TMEM147 Expression in Different Molecular or Immune Subtypes across Types of Cancer. To further explore the potential role of TMEM147 across cancers, we used data from the TISIDB database and found that TMEM147 was differentially expressed in different molecular subtypes of nine cancers and in different immune subtypes of 10 cancers. Among the molecular subtypes, TMEM147 was expressed at the highest levels in the CIMP-high subtype ($P = 2.99 \times 10^{-04}$) of ACC (Figure 2A), in the basal subtype ($P = 6.61\times 10^{-15}$) of BRCA (Figure 2B), in the classical subtype ($P = 2.19 \times 10^{-03}$) of

https://doi.org/10.1021/acsomega.4c01215
ACS Omega 2024, 9, 27137−27157

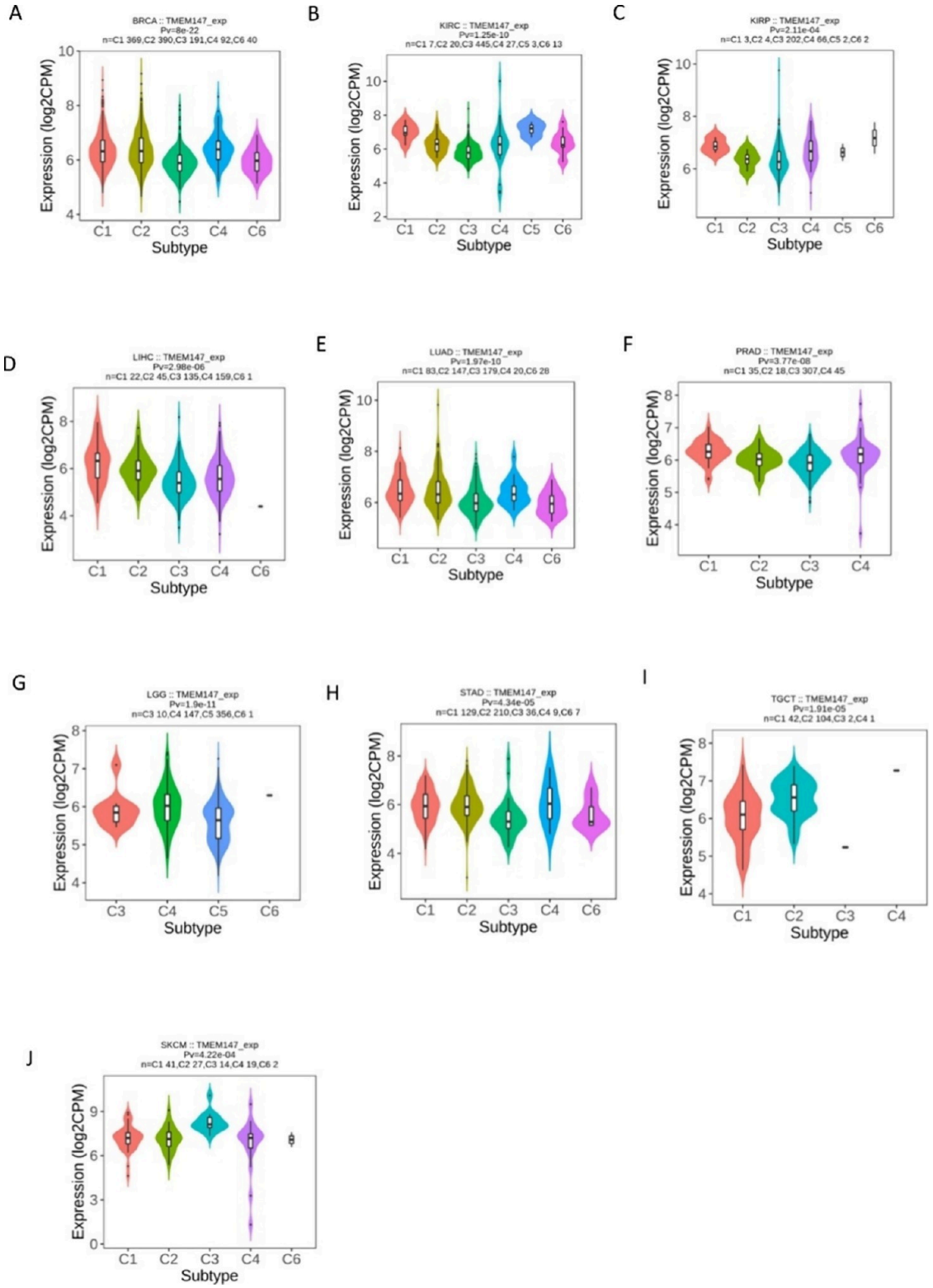

Figure 3. Correlations between TMEM147 expression and immune subtypes across tumors from the TCGA database. (A) BRCA; (B) KIRC; (C) KIRP; (D) LIHC; (E) LUAD; (F) PRAD; (G) LGG; (H) STAD; (I) TGCT; (J) SKCM.

HNSC (Figure 2C), in the C2b subtype ($P = 2.19 \times 10^{-03}$) of KIRP (Figure 2D), in the classic-like subtype ($P = 8.2 \times 10^{-55}$) of LGG (Figure 2E), in the iCluster subtype ($P = 1.03 \times 10^{-02}$) of HIHC (Figure 2F), in the ortical admixture subtype ($P = 2.33 \times 10^{-03}$) of PCPG (Figure 2G), in the HM-SNV subtype ($P = 3.74 \times 10^{-05}$) of STAD (Figure 2H), and in the CN-HIGH subtype ($P = 1.89 \times 10^{-03}$) of UCEC (Figure 2I).

Furthermore, regarding the immune subtypes, the expression of TMEM147 was related to different immune subtypes (C1: wound healing; C2: IFN-γ-dominant; C3: inflammatory; C4: lymphocyte-depleted; C5: immunologically quiescent; C6:

https://doi.org/10.1021/acsomega.4c01215
ACS Omega 2024, 9, 27137−27157

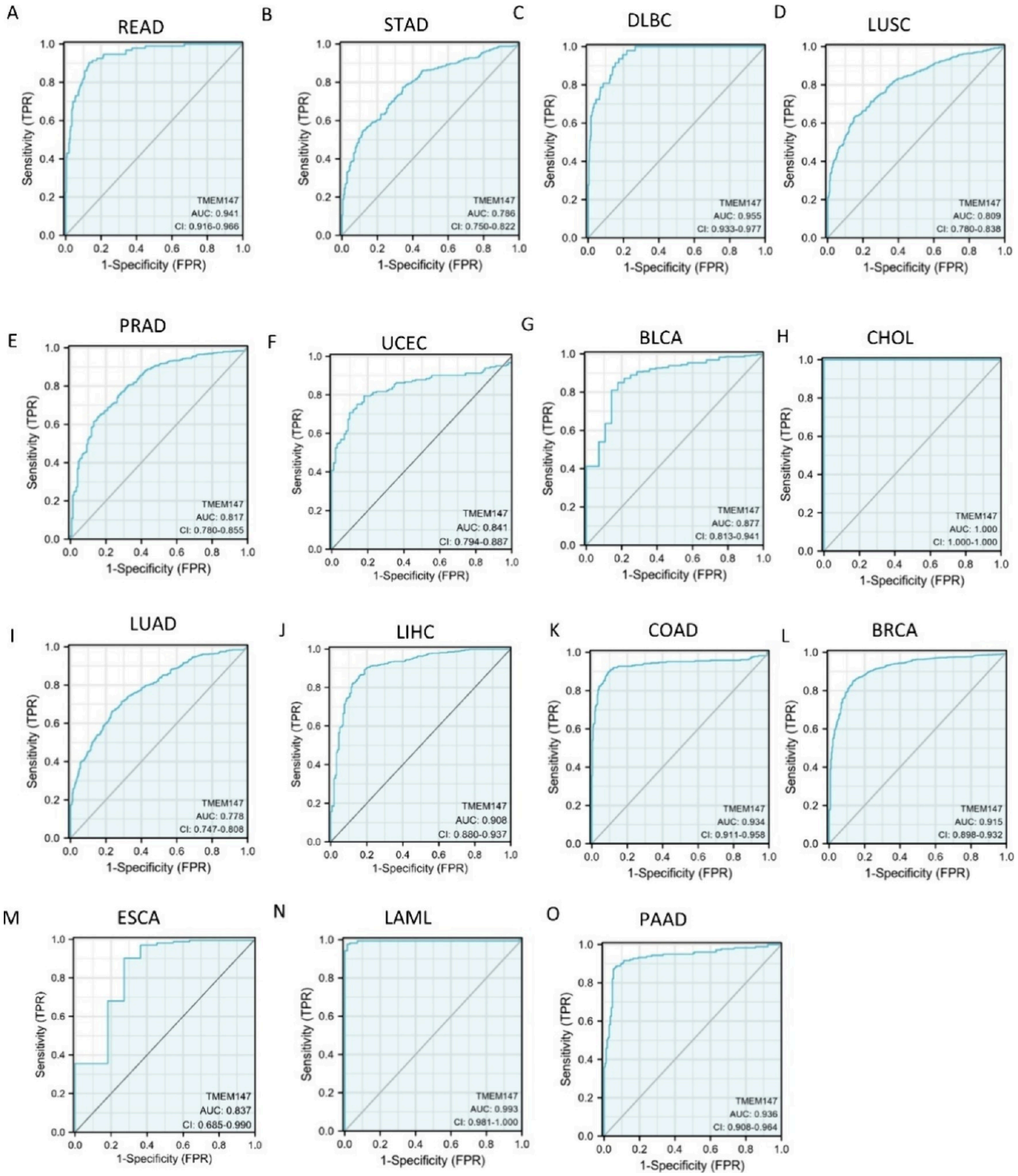

Figure 4. Receiver operating characteristic (ROC) curve for TMEM147 expression across cancers. (A) READ; (B) STAD; (C) DLBC; (D) LUSC; (E) PRAD; (F) UCEC; (G) BLCA; (H) CHOL; (I) LUAD; (J) LIHC; (K) COAD; (L) BRCA; (M) ESCA; (N) LAML; (O) PAAD.

TGF-b-dominant) of 10 cancers, including BRCA (Figure 3A), KIRC (Figure 3B), KIRP (Figure 3C), LIHC (Figure 3D), LIAD (Figure 3E), PRAD (Figure 3F), LGG (Figure 3G), STAD (Figure 3H), TGCT (Figure 3I), and SKCM (Figure 3J).

High Diagnostic Value of TMEM147 across Cancers. To confirm the diagnostic value of TMEM147 across cancers, we generated ROC curves using TCGA data. The ROC curves showed high predictive values (ROC > 0.7) of TMEM147 in 15 types of cancer, including READ (AUC = 0.941; CI = 0.916−0.966), STAD (AUC = 0.786; CI = 0.750−0.822), DLBC (AUC = 0.955; CI = 0.933−0.977), LUSC (AUC = 0.809; CI = 0.780−0.838), PRAD (AUC = 0.817; CI = 0.780−0.855), UCEC

https://doi.org/10.1021/acsomega.4c01215
ACS Omega 2024, 9, 27137−27157

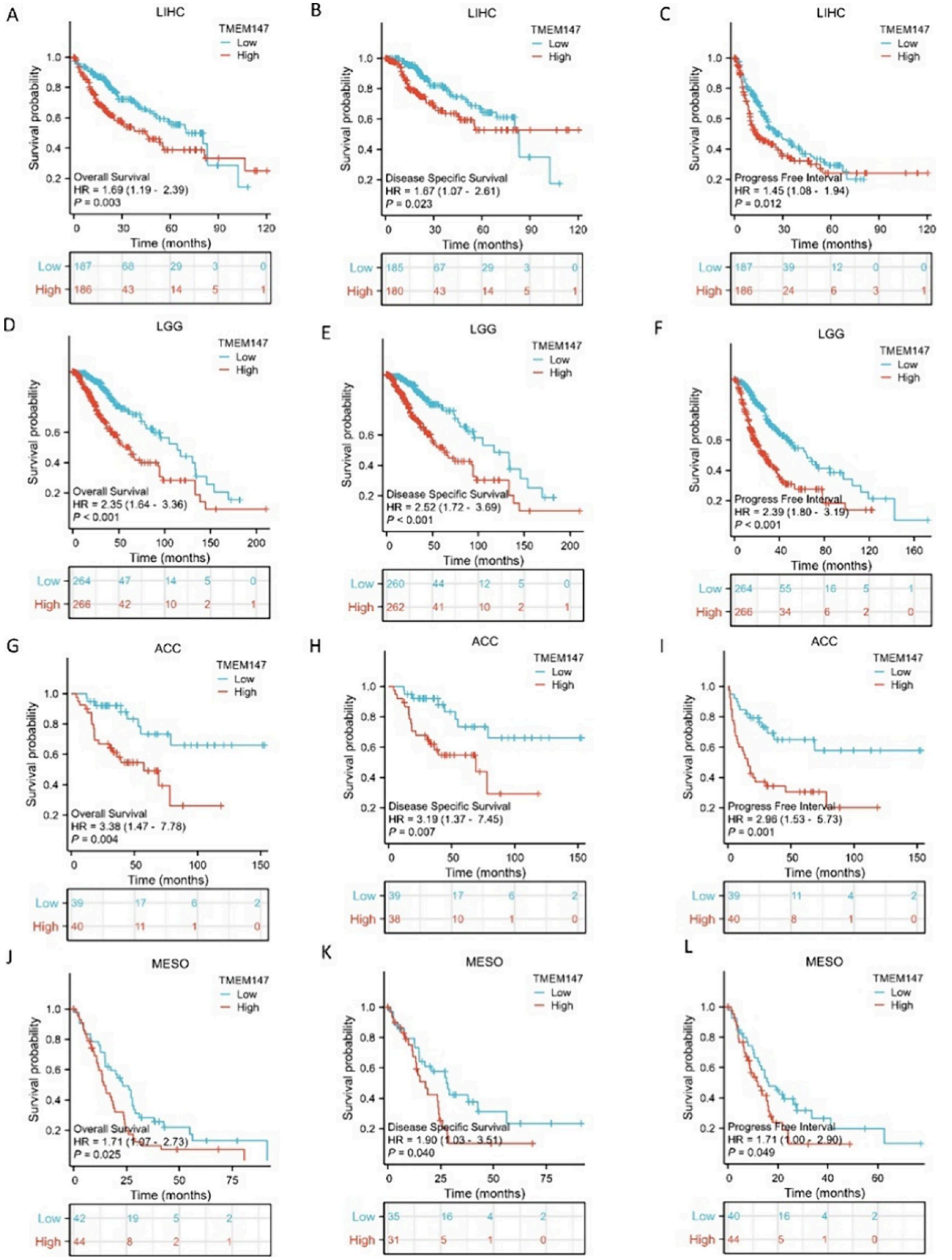

Figure 5. Correlations between TMEM147 expression and cancer patient prognosis (OS, DSS, and PFI). (A−C) LIHC; (D−F) LGG; (G−I) ACC; (J−L) MESO.

https://doi.org/10.1021/acsomega.4c01215
ACS Omega 2024, 9, 27137−27157

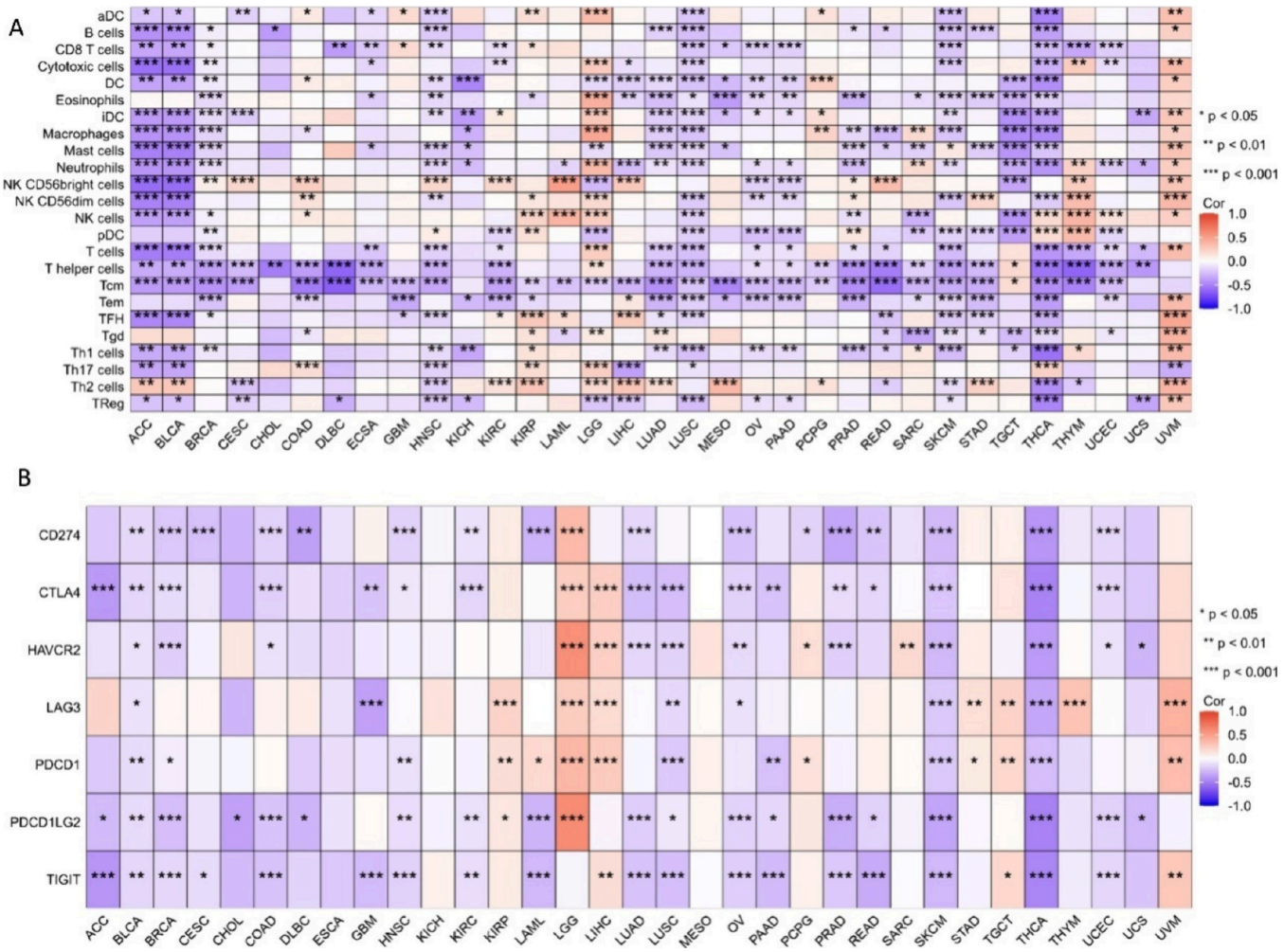

Figure 6. Correlation analysis of TMEM147 expression and immune cell infiltration across cancers. (A) Heatmap of the correlation of TMEM147 expression with 24 types of tumor-infiltrating immune cells. (B) Correlation analysis of TMEM147 expression and immune checkpoint expression in pan-cancer tissues.

(AUC = 0.841; CI = 0.794−0.887), BLCA (AUC = 0.877; CI = 0.813−0.941), CHOL (AUC = 1.000; CI = 1.000−1.000), LUAD (AUC = 0.778; CI = 0.747−0.808), LIHC (AUC = 0.908; CI = 0.880−0.937), COAD (AUC = 0.934; CI = 0.911−0.958), BRCA (AUC = 0.915; CI = 0.898−0.932), ESCA (AUC = 0.837; CI = 0.685−0.990), LAML (AUC = 0.933; CI = 0.981−1.000), and PAAD (AUC = 0.936; CI = 0.908−0.964) (Figure 4A−O).

TMEM147 Expression Was Correlated with the Prognosis of Patients with Different Cancers. To determine the prognostic role of TMEM147 across cancers, Kaplan−Meier analysis was performed, and the results showed that higher expression of TMEM147 predicted a lower probability of survival among patients with LICH (Figure 5A−C), LGG (Figure 5D−F), ACC (Figure 5G−I), and MESO (Figure 5J−L). The TMEM147 expression level was correlated with the OS, DSS, and PFI of patients with these types of cancer.

TMEM147 Expression Was Correlated with Immune Cell Infiltration in Tumors. Infiltrating immune cells can recognize and attack cancer cells to suppress tumor growth and metastasis. Activation of the immune system helps to control tumor development and results in better prognosis. In our study, we investigated the relationship between TMEM147 expression and infiltrating immune cells. The heatmap showed that in most tumors, the expression of TMEM147 was negatively correlated with the infiltration of T helper cells and Tcm cells (Figure 6A). Immune checkpoint-related genes play a role in regulating the antitumor immune response and affect the immune escape and progression of tumors in patients with liver cancer. Typically, immune checkpoint molecules balance the immune response and prevent overactivated immune cells from damaging normal tissues. We studied the relationships between the expression of six immune checkpoint genes (CD274, CTLA4, HAVCR2, LAG3, PDCD1, PDCD1LG2, and TIGIT) and TMEM147. Our results showed that TMEM147 expression was almost negatively correlated with immune checkpoint-related gene expression in BLCA, OV, SKCM, and THCA and positively correlated with immune checkpoint gene expression in LGG and LIHC, suggesting that TMEM147 is related to immune escape in cancer (Figure 6B).

Gene Functional Enrichment Analysis of TMEM147 across Cancers. To investigate the mechanism by which TMEM147 functions during tumorigenesis, PPI network analysis was performed by utilizing the STRING database and Cytoscape. As shown in Figure 7A, an interaction network of 50 TMEM147-binding proteins that were identified by experimental evidence was visualized. GO enrichment analysis of the 50 TMEM147-binding proteins was conducted (Figure 7B),

https://doi.org/10.1021/acsomega.4c01215
ACS Omega 2024, 9, 27137−27157

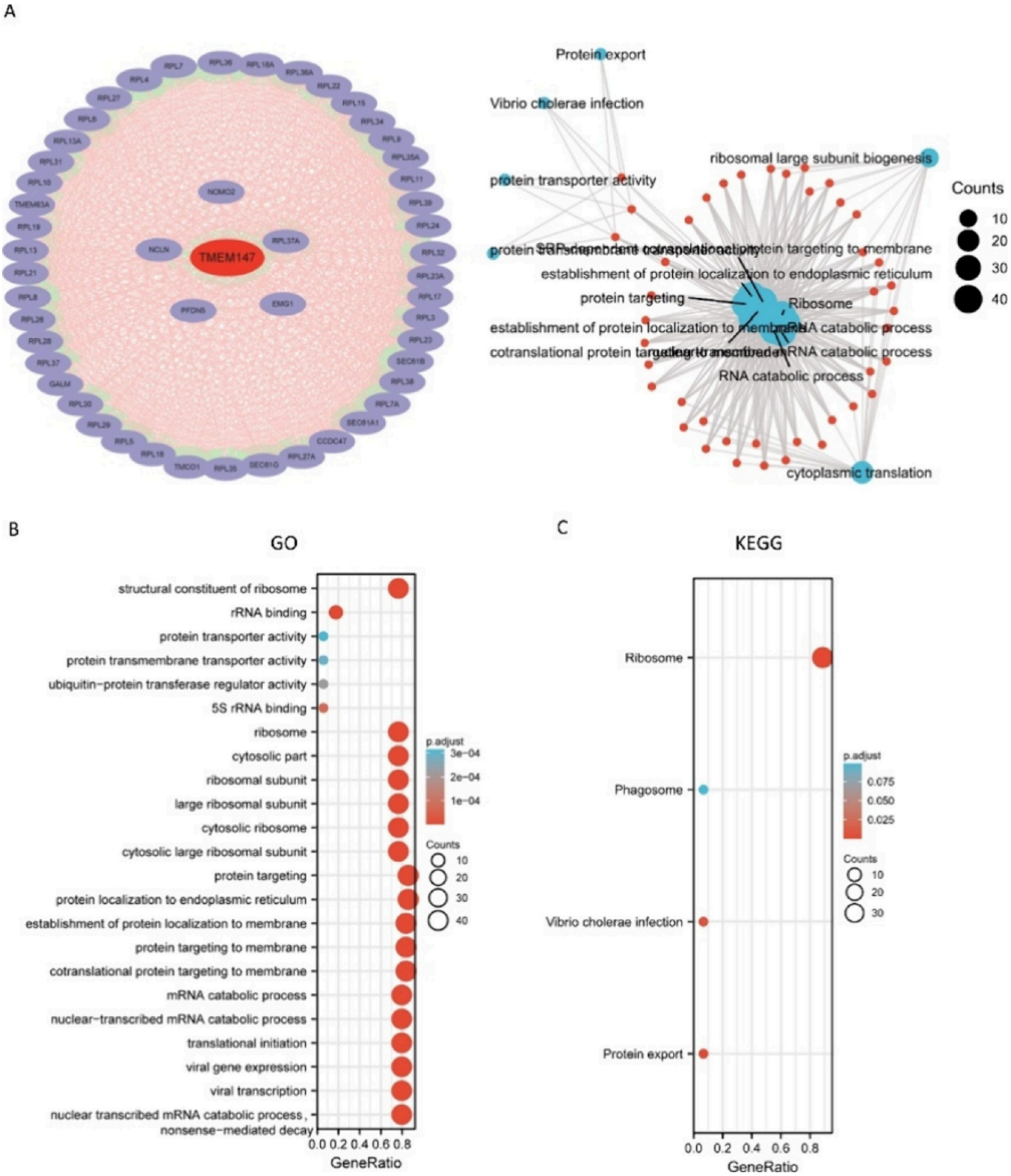

Figure 7. PPI network, GO analysis, and KEGG analysis of 50 TMEM147-binding proteins. (A) PPI network; (B) visual network of GO and KEGG analyses; (C) GO analysis; (D) KEGG analysis.

and the results showed that 19 pathways were enriched, including the structural constituent of ribosome, rRNA binding, protein transporter activity, protein transmembrane transporter activity, ubiquitin-protein transferase regulator activity, 5S rRNA binding, ribosome, cytosolic part, ribosomal subunit, large ribosomal subunit, cytosolic ribosome, cytosolic large ribosomal subunit, protein targeting, protein localization to endoplasmic reticulum, establishment of protein localization to membrane, protein targeting to membrane, cotranslational protein targeting to the membrane, mRNA catabolic process, nuclear-transcribed mRNA catabolic process, translational initiation, viral gene expression, viral transcription, nuclear-

https://doi.org/10.1021/acsomega.4c01215
ACS Omega 2024, 9, 27137−27157

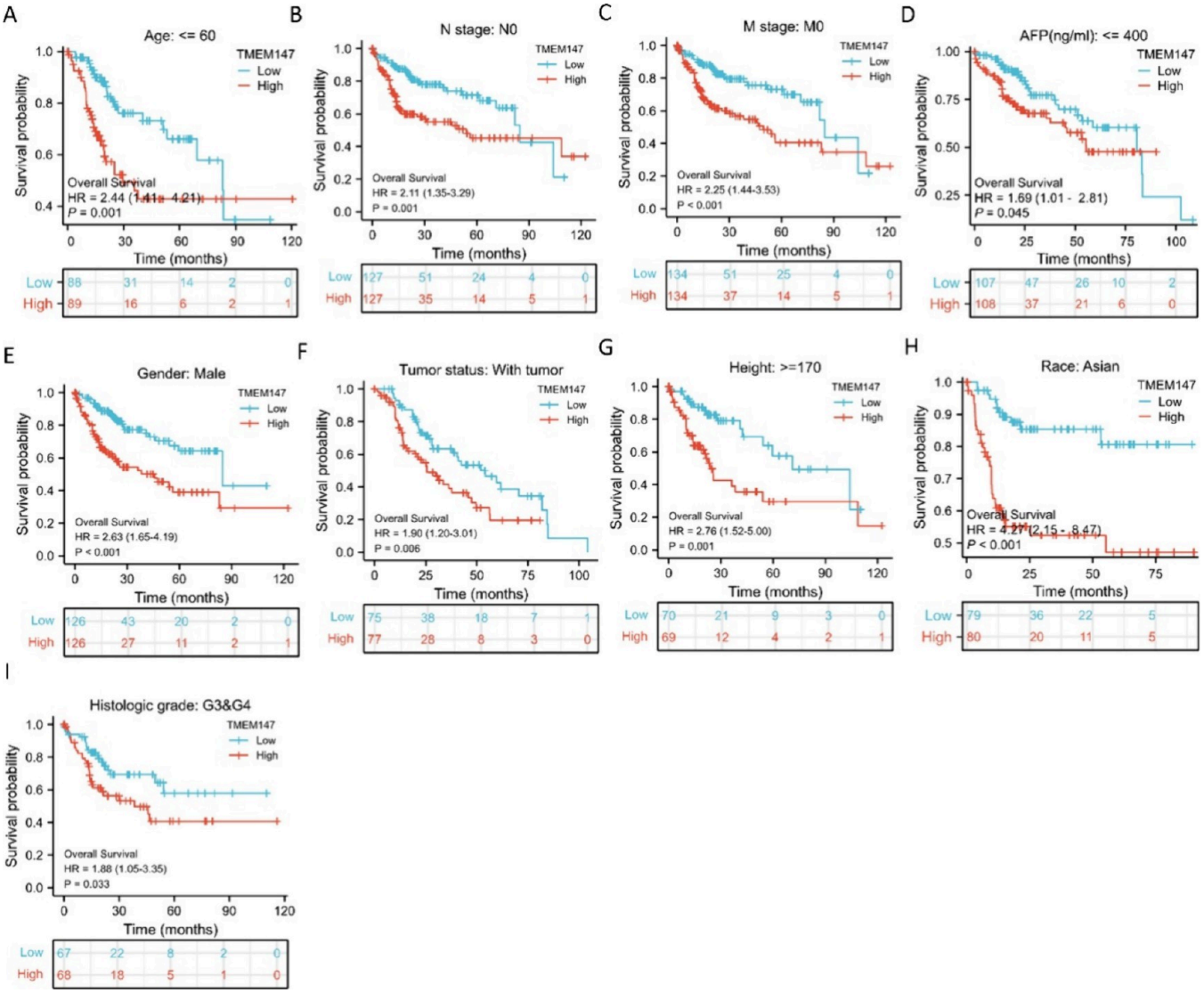

Figure 8. Associations between TMEM147 expression and OS in different clinical subgroups of patients with LIHC. (A) Age > 60; (B) N stage: N0; (C) M stage: M0; (D) AFP (ng/mL): >400; (E) sex: male; (F) tumor status: positive; (G) height: >170; (H) race: Asian; (I) histological grade: G3 and G4.

transcribed mRNA catabolic process, and nonsense-mediated decay (Figure 7C). KEGG pathway enrichment analysis revealed that the most highly enriched pathways were ribosome, phagosome, *Vibrio cholerae* infection, and protein export.

High TMEM147 Expression Was Correlated with Poor Prognosis in Patients with Different Clinical Characteristics. According to the results of the pan-cancer study described above, TMEM147 was differentially expressed in liver cancer and may be used as a biomarker for liver cancer; therefore, we conducted a more in-depth study on LIHC. The higher expression of TMEM147 was associated with worse OS in patients with the following characteristics: age ≤ 60 years (Figure 8A); N stage: N0 (Figure 8B); M stage: M0 (Figure 8C); AFP (ng/mL): 400 (Figure 8D); sex: male (Figure 8E); tumor status: positive (Figure 8F); height ≥ 170 (Figure 8G); race: Asian (Figure 8H); histological grade: G3 and G4 (Figure 8I). The higher expression of TMEM147 was associated with worse DSS in patients with the following characteristics: tumor status: positive (Figure 9A); race: Asian (Figure 9B); pathological M stage: M0 (Figure 9C); pathological N stage: N0 (Figure 9D); sex: male (Figure 9E); histological type: hepatocellular carcinoma (Figure 9F). The higher expression of TMEM147 was associated with worse PFI in patients with the following characteristics: M stage: M0 (Figure 10A); tumor status: positive (Figure 10B); race: Asian (Figure 10C); pathological N stage: N0 (Figure 10D); age ≤ 60 years (Figure 10E); height ≥ 170 (Figure 10F).

TMEM147 Expression Was Correlated with the Clinicopathological Characteristics of LICH Patients. The associations between the expression of TMEM147 and the clinical characteristics of LICH patients were explored, and the results are shown in Table 2. AFP (ng/mL) ($P < 0.001$), BMI ($P = 0.019$), weight ($P = 0.002$), OS ($P = 0.002$), T stage ($P = 0.005$), pathological stage ($P = 0.004$), and histological grade ($P < 0.001$) were significantly related to TMEM147 expression.

Moreover, the results of Welch one-way ANOVA revealed that TMEM147 was highly expressed in the tumor-positive group (Figure 11A), in the AFP > 400 ng/mL group (Figure 11B), in the BMI ≤ 25 group (Figure 11C), in the weight ≤70 kg group (Figure 11D), in the Dead group (Figure 11E), in the T2

https://doi.org/10.1021/acsomega.4c01215
ACS Omega 2024, 9, 27137−27157

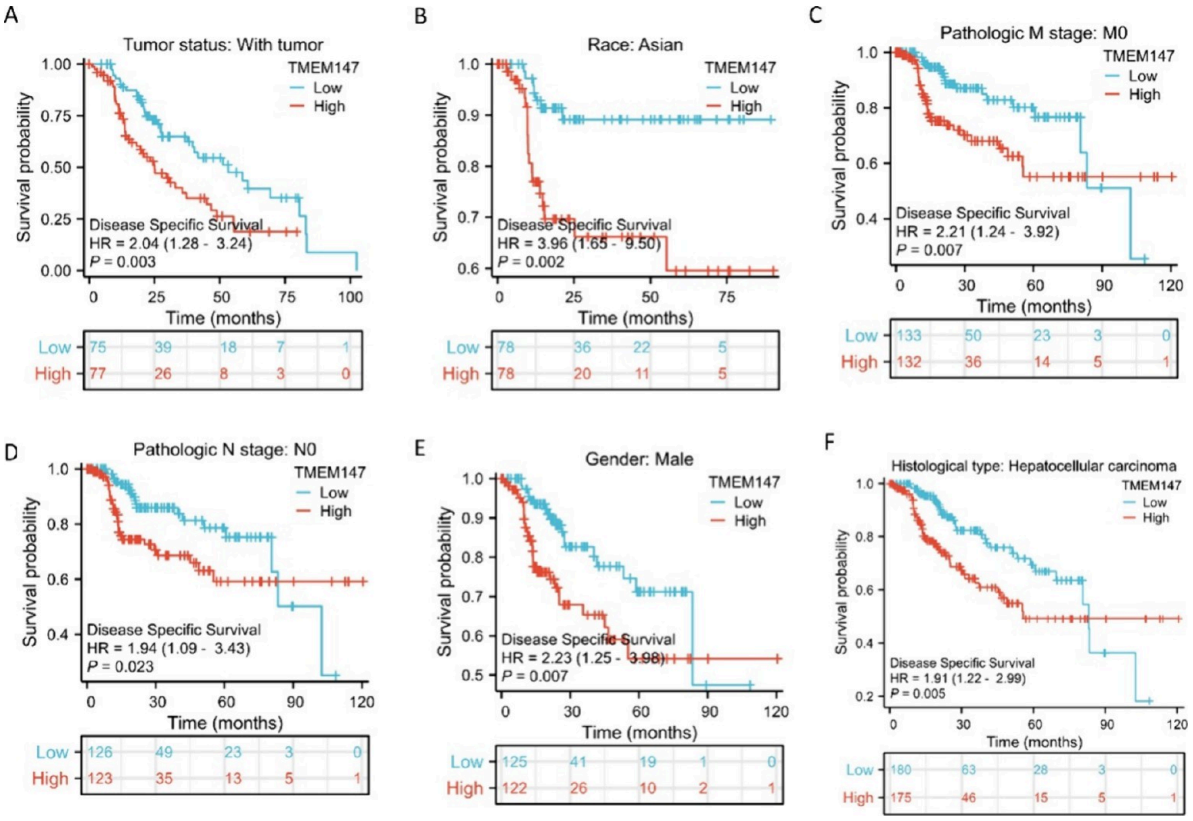

Figure 9. Associations between TMEM147 expression and DSS in different clinical subgroups of LIHC patients. (A) Tumor status: positive; (B) race: Asian; (C) pathological M stage: M0; (D) pathological N stage: N0; (E) sex: male; (F) histological type: hepatocellular carcinoma.

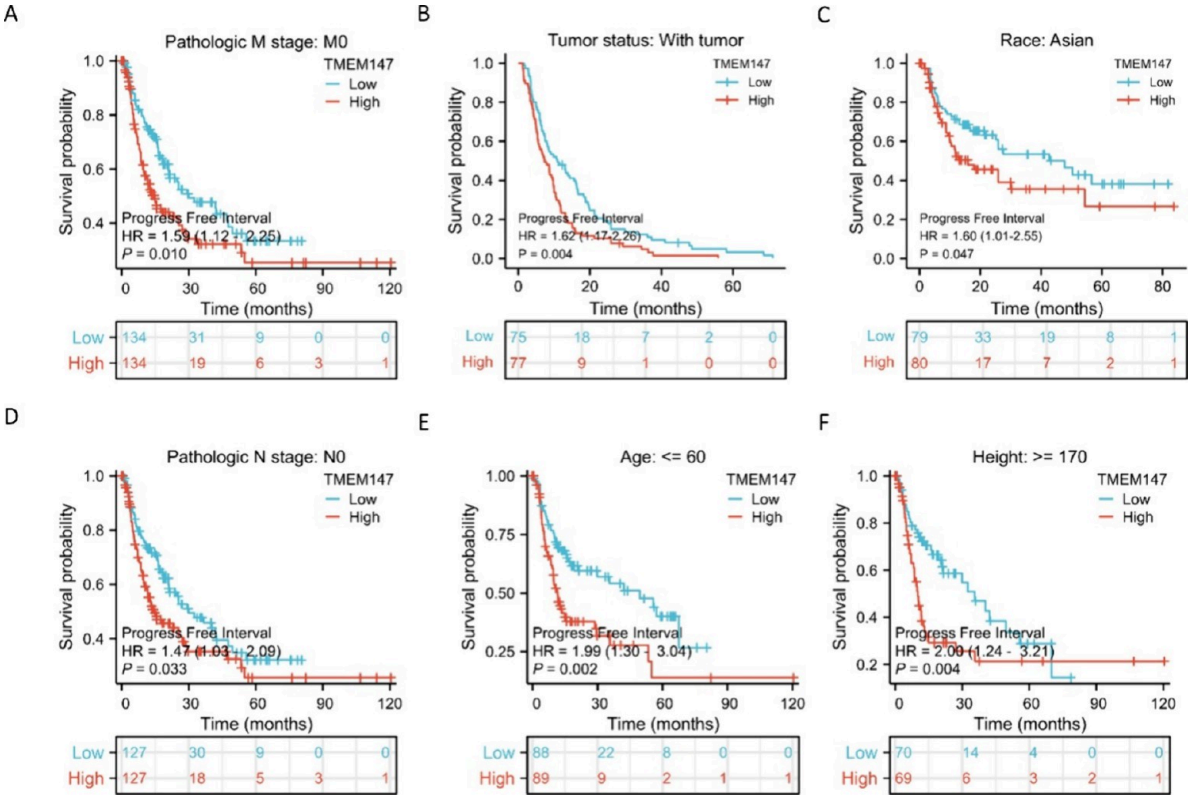

Figure 10. Associations between TMEM147 expression and the PFI in different clinical subgroups of LIHC patients. (A) M stage: M0; (B) tumor status: positive; (C) race: Asian. (D) pathological N stage: N0. (E) Age $\leq$ 60 years; (F) height $\geq$ 170.

https://doi.org/10.1021/acsomega.4c01215
ACS Omega 2024, 9, 27137−27157

Table 2. Clinical Characteristics of LIHC Patients

characteristic	low expression of TMEM147	high expression of TMEM147	*P* value
n	187	187	
tumor status, *n* (%)			0.163
tumor-free	110 (31%)	92 (25.9%)	
with tumor	71 (20%)	82 (23.1%)	
AFP (ng/mL), *n* (%)			<0.001
≤400	123 (43.9%)	92 (32.9%)	
>400	20 (7.1%)	45 (16.1%)	
BMI, *n* (%)			0.019
≤25	77 (22.8%)	100 (29.7%)	
>25	91 (27%)	69 (20.5%)	
weight, *n* (%)			0.002
≤70	78 (22.5%)	106 (30.6%)	
>70	96 (27.7%)	66 (19.1%)	
OS event, *n* (%)			0.002
alive	137 (36.6%)	107 (28.6%)	
dead	50 (13.4%)	80 (21.4%)	
T stage, *n* (%)			0.005
T1	108 (29.1%)	75 (20.2%)	
T2	41 (11.1%)	54 (14.6%)	
T3	30 (8.1%)	50 (13.5%)	
T4	6 (1.6%)	7 (1.9%)	
pathological stage, *n* (%)			0.004
stage I	103 (29.4%)	70 (20%)	
stage II	38 (10.9%)	49 (14%)	
stage III	34 (9.7%)	51 (14.6%)	
stage IV	1 (0.3%)	4 (1.1%)	
histological grade, *n* (%)			<0.001
G1	35 (9.5%)	20 (5.4%)	
G2	102 (27.6%)	76 (20.6%)	
G3	43 (11.7%)	81 (22%)	
G4	5 (1.4%)	7 (1.9%)	
age, median (IQR)	62 (54, 69)	60 (50, 68)	0.123

stage group (Figure 11F), and in the G2, G3, and G4 groups (Figure 11G) compared with the control group.

Analysis of Molecules that Were Correlated with TMEM147 in LIHC Patients. Using data from the TCGA database, we identified 50 genes that were most highly positively or negatively related to TMEM147 in LIHC. Figure 12A shows the gene coexpression heatmap of the top 50 positively correlated genes, and the scatter plot shows that CNPAS1 (r = 0.740) (Figure 12B), RFXANK (r = 0.742) (Figure 12C), SMG9 (r = 0.718) (Figure 12D), EIF3K (r = 0.712) (Figure 12E), TOMM40 (r = 0.730) (Figure 12F), SNRPD2 (r = 0.768) (Figure 12G), PPP2R1A (r = 0.745) (Figure 12H), GSK3A (r = 0.719) (Figure 12I), TMM50 (r = 0.744) (Figure 12J), and UBE2M (Figure 12K) (r = 0.750) were the top 10 positively related genes. Moreover, the heatmap of negatively related genes (Figure 13A) revealed the top 10 genes, which included ABAT (r = −0.617) (Figure 13B), C8A (r = −0.614) (Figure 13C), DMGDH (r = −0.587) (Figure 13D), EHHADH (r = −0.600) (Figure 13E), CYP8B1 (r = −0.581) (Figure 13F), F11 (r = −0.584) (Figure 13G), PFKFB1 (r = −0.565) (Figure 14H), GLYATL1 (r = −0.587) (Figure 13I), ACSM2A (r = −0.603) (Figure 13J), and GYS2 (r = −0.647) (Figure 13K).

Differentially Expressed Genes (DEGs) Between LIHC Samples with High TMEM147 Expression and LIHC Samples with Low TMEM147 Expression. To elucidate gene expression profiles, ggplot2 was used to identify sets of genes that were significantly up- and downregulated. Using |log (fold change)| > 1 and adjusted *P* value <0.05 as cutoff criteria, a total of 3818 upregulated genes and 1408 downregulated genes were identified (Figure 14A). Then, we conducted GSEA and GO and KEGG enrichment analyses (Figure 14B−D) of the DEGs, and the GSEA results revealed that genes that are related to arachidonic acid metabolism, butanoate metabolism, drug metabolism, cytochrome p450, drug metabolism, other enzymes, fatty acid metabolism, and metabolism of xenobiotics by cytochrome p450 were enriched (Figure 14B). GO analysis revealed that the fatty acid catabolic process, fatty acid oxidation, lipid oxidation, regulation of chromosome segregation, lipid modification, membrane lipid metabolic process, branched-chain amino acid metabolic process, lipid catabolic process, sphingolipid metabolic process, membrane lipid biosynthetic process, and fatty acid metabolic process were enriched in BP, the chromosomal region was enriched in CC, and transferase activity, transferring acyl groups, coenzyme binding, and fatty acid binding were enriched in MF (Figure 14C). The KEGG pathway enrichment showed that the DEGs were mainly related to propanoyl-CoA metabolism, propanoyl-CoA, beta-oxidation, and fatty acid degradation (Figure 14D).

Analysis of the Association between TMEM147 Expression and Immune Cell Infiltration in LIHC. To better confirm the association between immune cell infiltration and TMEM147 expression in LIHC, the ssGSEA immuno-infiltration algorithm in GSVA was used. The Wilcoxon rank sum test showed that TH2 cells, TFH cells, and NK CD56 bright cells were significantly positively correlated with the expression of TMEM147 (P < 0.001) (Figure 15A). The scatter plots in Figure 15B show that Th2 cells (r = 0.318, P < 0.001), TFH cells (r = 0.285, P < 0.001), and NK CD56 bright cells (r = 0.280, P < 0.001) show this positive correlation, but no significant associations were observed for macrophages, activated dendritic cells (aDCs), or Th1 cells. Moreover, Th17 cells, Tcm cells, neutrophils, Tregs, DCs, and cytotoxic cells were significantly negatively associated with TMEM147 expression (Figure 16A). The scatter plots in Figure 16B show this negative correlation of Th17 cells (r = 0.275, P < 0.001), Tcm cells (r = 0.260, P < 0.001), neutrophils (r = 0.217, P < 0.001), Tregs (r = 0.185, P < 0.001), DCs (r = 0.182, P < 0.001), and cytotoxic cells (r = 0.144, P = 0.005) with TMEM147 expression.

TMEM147 Promoted Cell Proliferation in Liver Cancer. PCR and western blotting experiments revealed that TMEM147 was overexpressed in liver cancer cells, with higher expression levels observed in HepG2 and Huh-7 cells (Figure 17A,B). Subsequent investigations were performed using the HepG2 and Huh-7 cell lines. Four siRNAs were designed and used to knock down TMEM147 expression in the cells, and the results demonstrated that siRNA-4 most effectively knocked down TMEM147 expression in HepG2 cells, while siRNA-3 had the greatest effect on Huh-7 cells (Figure 17C). CCK-8 and colony formation assays indicated a significant reduction in cell proliferation after TMEM147 knockdown (Figure 17D,E). Moreover, EDU experiments demonstrated that downregulation of TMEM147 reduced DNA replication in cells, thereby affecting cell proliferation (Figure 17F).

DISCUSSION

Cancer is a major public health problem worldwide, and it is the second leading cause of death in the United States.[17]

https://doi.org/10.1021/acsomega.4c01215
ACS Omega 2024, 9, 27137−27157

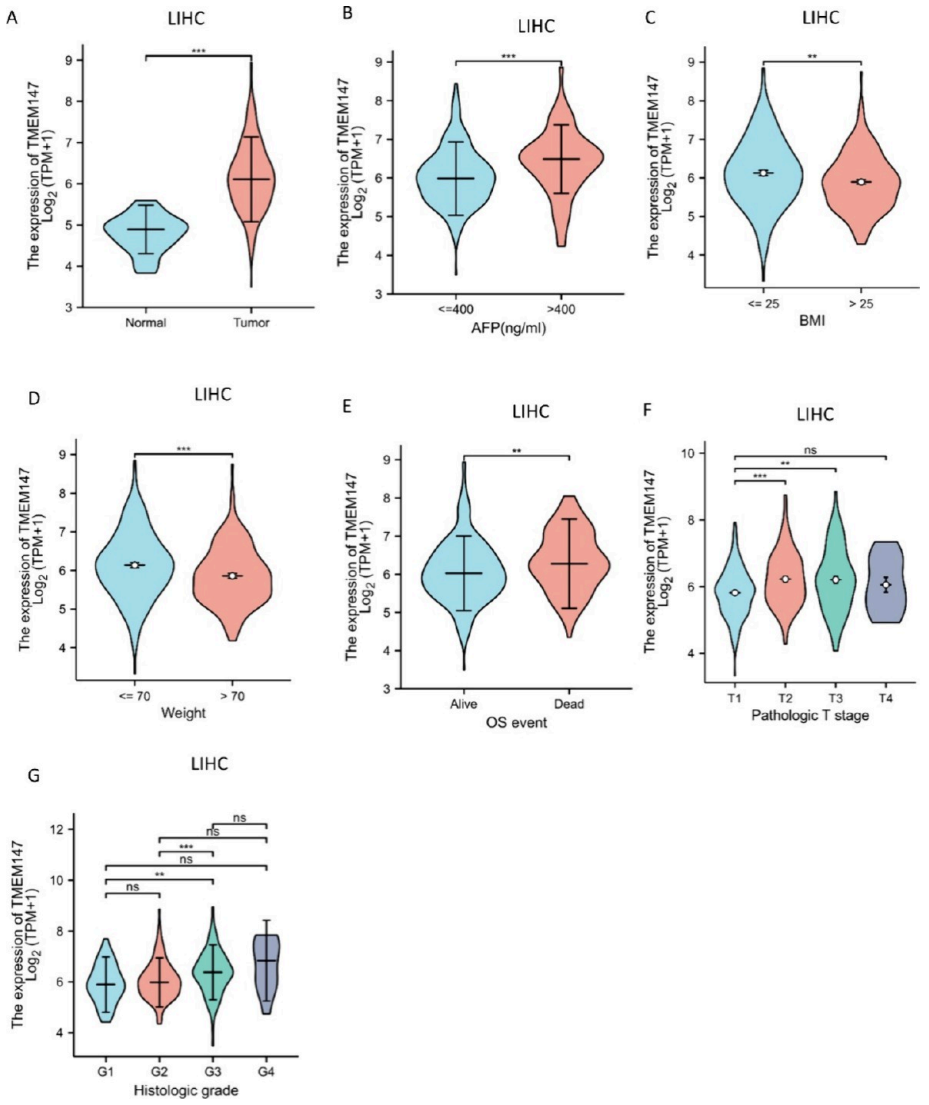

Figure 11. Associations between TMEM147 expression and different clinical characteristics in LIHC patients. (A) Tumor status; (B) AFP; (C) BMI; (D) weight; (E) OS; (F) T stage; (G) pathological stage; (H) histological grade. ns, $P \geq 0.05$; *$P < 0.05$; **$P < 0.01$; ***$P < 0.001$.

Researchers have continuously worked to develop treatments for cancer. Currently, there are many methods and approaches for treating tumors, such as surgery, radiotherapy, chemotherapy, biological therapy, and immunotherapy; each of these methods is efficacious and has its own advantages. However, investigations of tumor biomarkers are still very limited, and further research is warranted.

The TMEM family is a group of proteins that span the entire width of the lipid bilayer and are permanently anchored in membranes. Many TMEMs act as channels, allowing the transport of specific substances across biological membranes.[18] Because they allow specific substances to be transported through biofilms, facilitate communication between intracellular and extracellular spaces, and perform other unknown biological functions, TMEM family members play important roles in the migration, metastasis, and progression of a variety of tumors.[19,20] TMEM45A and TMEM205 have been implicated in tumor progression and invasion but also in tumor chemoresistance.[21] Few studies have systematically explored the expression of TMEM147, which is a member of the TMEM family, across cancers via bioinformatics. This study aimed to investigate the role of TMEM147 across cancers and to use LIHC as a specific example to illustrate the potential value of TMEM147.

In the present study, by using high-throughput RNA sequencing data, we found that TMEM147 is differentially expressed across cancers, and ROC curves of TMEM147 expression in 15 kinds of cancer revealed a high AUC, indicating that TMEM147 might be a potential diagnostic biomarker. The heterogeneity or intrinsic diversity of cancer is the main reason why cancers can adapt to pharmacological pressures and then evolve;[22] for instance, LIHC is a heterogeneous disease at both the molecular and histological levels.[23] Heterogeneity is a major obstacle to the development of effective targeted therapies, and studying the heterogeneity of tumors can help clinicians implement individualized and differential treatments for patients.[24,25] The subtype analysis in our study revealed that TMEM147 was differentially expressed in many molecular and immune subtypes of cancer, which may provide directions for treatment in the context of tumor heterogeneity. Notably, TMEM147 is closely correlated with both molecular and immune subtypes in BRCA, KIRP, LGG, LIHC, and STAD. Furthermore, Kaplan−Meier survival curves confirmed the high prognostic value of TMEM147 among patients with LIHC,

https://doi.org/10.1021/acsomega.4c01215
ACS Omega 2024, 9, 27137−27157

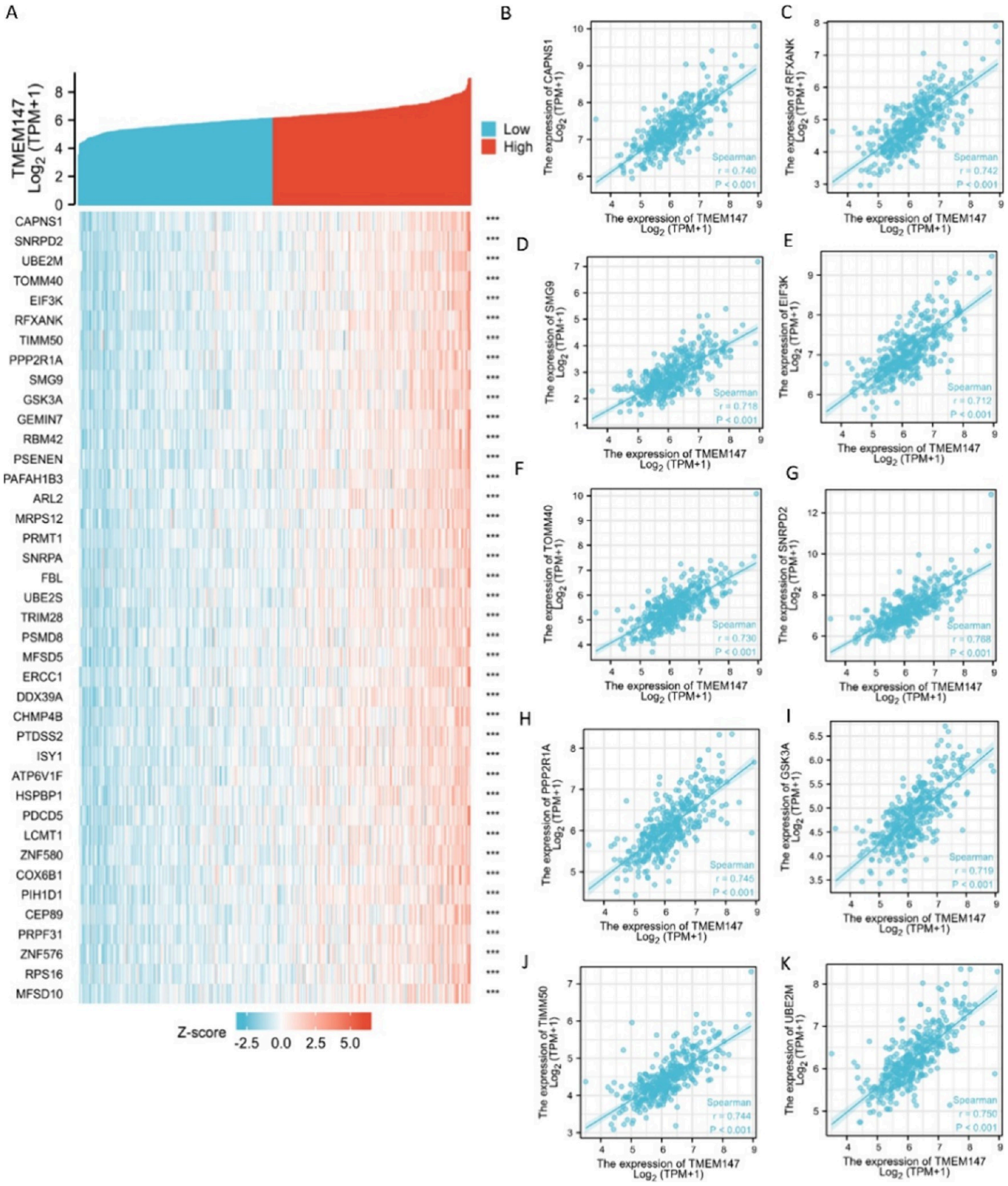

Figure 12. Top 50 genes that were positively correlated with TMEM147 expression in LIHC. (A) Gene coexpression heatmap of the top 50 genes that were positively correlated with TMEM147 in LIHC; (B−K) correlation analysis of the top 10 genes that were positively correlated with TMEM147 in the heatmap.

LGG, ACC, and MESO. This result shows that TMEM147 could be a biomarker for the prognosis of patients with different kinds of cancer. To further understand the role of TMEM147 across cancers, enrichment analysis of 50 TMEM147-binding proteins was performed. The results revealed that ribosome-related functions and membrane protein-related functions, which are associated with the transmembrane protein activity

https://doi.org/10.1021/acsomega.4c01215
ACS Omega 2024, 9, 27137−27157

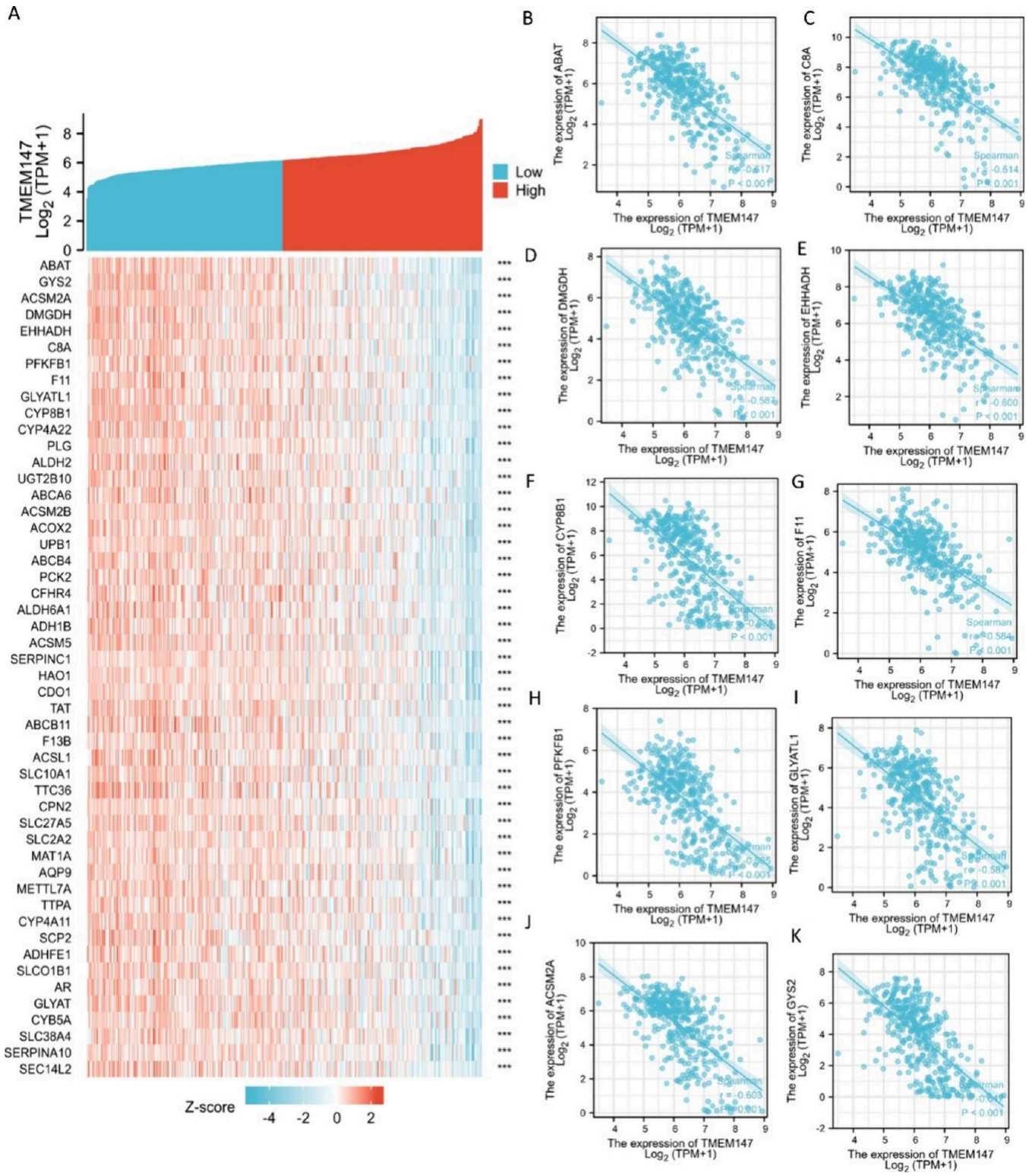

Figure 13. Top 50 genes that were negatively correlated with TMEM147 expression in LIHC. (A) Gene coexpression heatmap of the top 50 genes that were negatively correlated with TMEM147 in LIHC; (B−K) correlation analysis of the top 10 genes that were negatively correlated with TMEM147 in the heatmap.

of TMEM147, were highly enriched. These results demonstrated the potential role of TMEM147 across cancers.

Among all malignant diseases, liver cancer is the fourth most common cause of cancer-related deaths worldwide and ranks sixth in terms of incidence.[26] Viral hepatitis, alcoholism, and fungal toxin exposure are major risk factors for the development of liver cancer, but in recent years, obesity, insulin resistance, and type 2 diabetes-associated fatty liver disease (NAFLD) have been recognized as triggers of liver cancer, especially in developed countries.[27] Despite its prevalence and high mortality rate, reliable treatments to reduce mortality are still scarce,[28] and predictive biomarkers are urgently needed to inform the

https://doi.org/10.1021/acsomega.4c01215
ACS Omega 2024, 9, 27137−27157

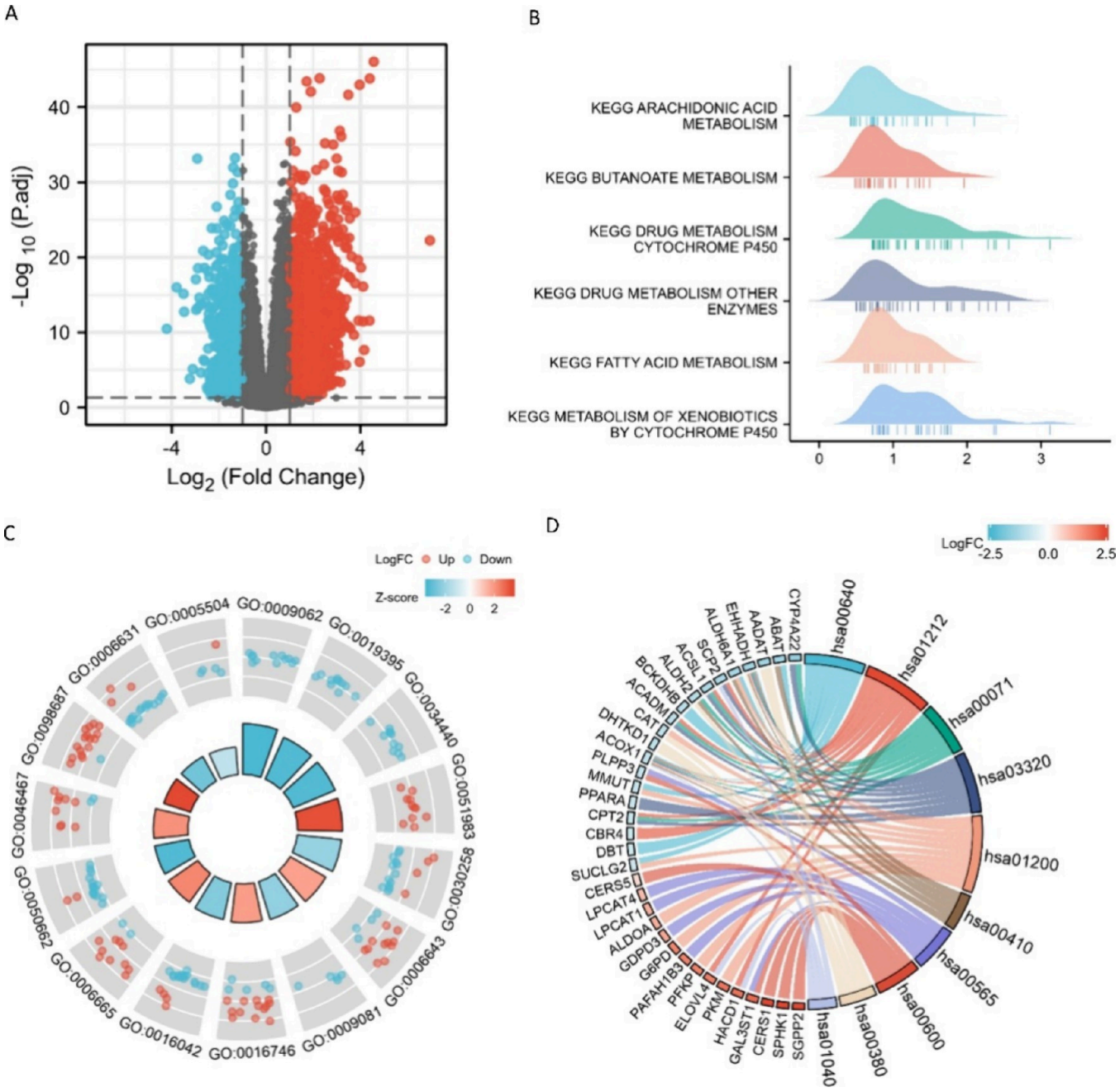

Figure 14. PPI network construction and GO and KEGG analyses of DEGs between LIHC samples with high TMEM147 expression and LIHC samples with low TMEM147 expression. (A) Volcano map of DEGs (red: upregulated; blue: downregulated); (B) GSEA; (C, D) GO and KEGG analyses of DEGs.

selection of molecular and immune-based treatments in addition to surgery, liver transplantation, and local ablative and intra-arterial therapies.[29]

In addition to poor prognosis of patients with different kinds of cancers, multiple clinical subgroups of patients with LIHC who also had high TMEM147 expression had poor DSS and PFI. Moreover, the expression of TMEM147 differed according to different clinical characteristics. More importantly, in the functional analysis, the KEGG, GO, and GSEA analyses revealed enrichment of metabolism-related pathways, such as fatty acid metabolism, arachidonic acid metabolism, lipid modification, and membrane lipid metabolic processes. Abnormal metabolic processes, including abnormal levels of lipid metabolism, can affect tumor metastasis, recurrence, and drug resistance and induce tumor immune evasion by influencing the antitumor response of immune cells.[30] In the tumor microenvironment, T cells, macrophages, DCs, NK cells, and other immune cells can regulate immune checkpoints, resulting in the inhibition of tumor cell elimination.[31] The liver is a major regulatory organ that manages metabolism throughout the body and maintains metabolic homeostasis; once metabolic homeostasis is disrupted, a variety of cancers, including LIHC, may occur.[32] Previous studies have shown that disorders of glucose metabolism,[33] lipid metabolism,[34] and nucleotide metabolism[35] may lead to the occurrence of liver cancer via different pathways. Understanding the changes that occur in the metabolic profile during hepatocarcinogenesis is important for elucidating the pathogenic mechanisms of cancer and identifying new

https://doi.org/10.1021/acsomega.4c01215
ACS Omega 2024, 9, 27137−27157

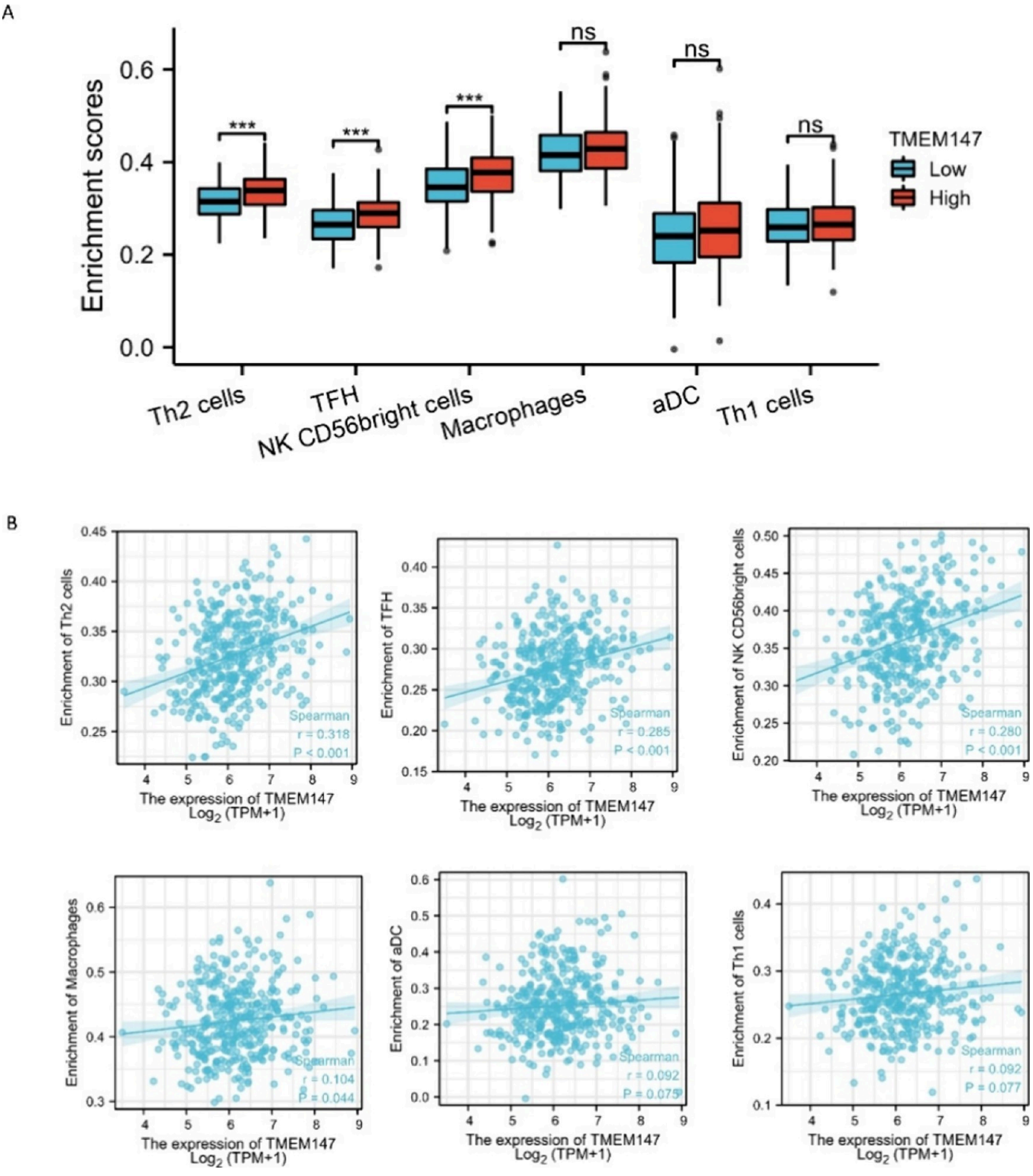

Figure 15. Analysis of the association of immune cell infiltration with TMEM147 expression in LIHC revealed 6 immune cell types that were positively related to TMEM147 expression. (A) Enrichment scores of TMEM147 expression in Th2 cells, TFH cells, NK CD56 bright cells, macrophages, aDCs, and Th1 cells. Correlation between TMEM147 expression and Th2 cells, TFH cells, NK CD56 bright cells, macrophages, aDCs, and Th1 cells (B); ns, $P \geq 0.05$; *$P < 0.05$; **$P < 0.01$; ***$P < 0.001$.

diagnostic and prognostic biomarkers. In our study, analysis of the correlation between TMEM147 expression and immune cell infiltration in LIHC revealed that TMEM147 was positively related to Th2 cells, TFH cells, and NK CD56 bright cells and negatively related to Th17 cells, Tcm cells, neutrophils, Tregs, DCs, and cytotoxic cells. Experiments that were performed with the normal human liver cell line MIHA and four LIHC cell lines (BEL-7402, SMMC-7721, HepG2, and Huh7 cells) confirmed the role of TMEM147 in promoting liver cancer cell

https://doi.org/10.1021/acsomega.4c01215
ACS Omega 2024, 9, 27137−27157

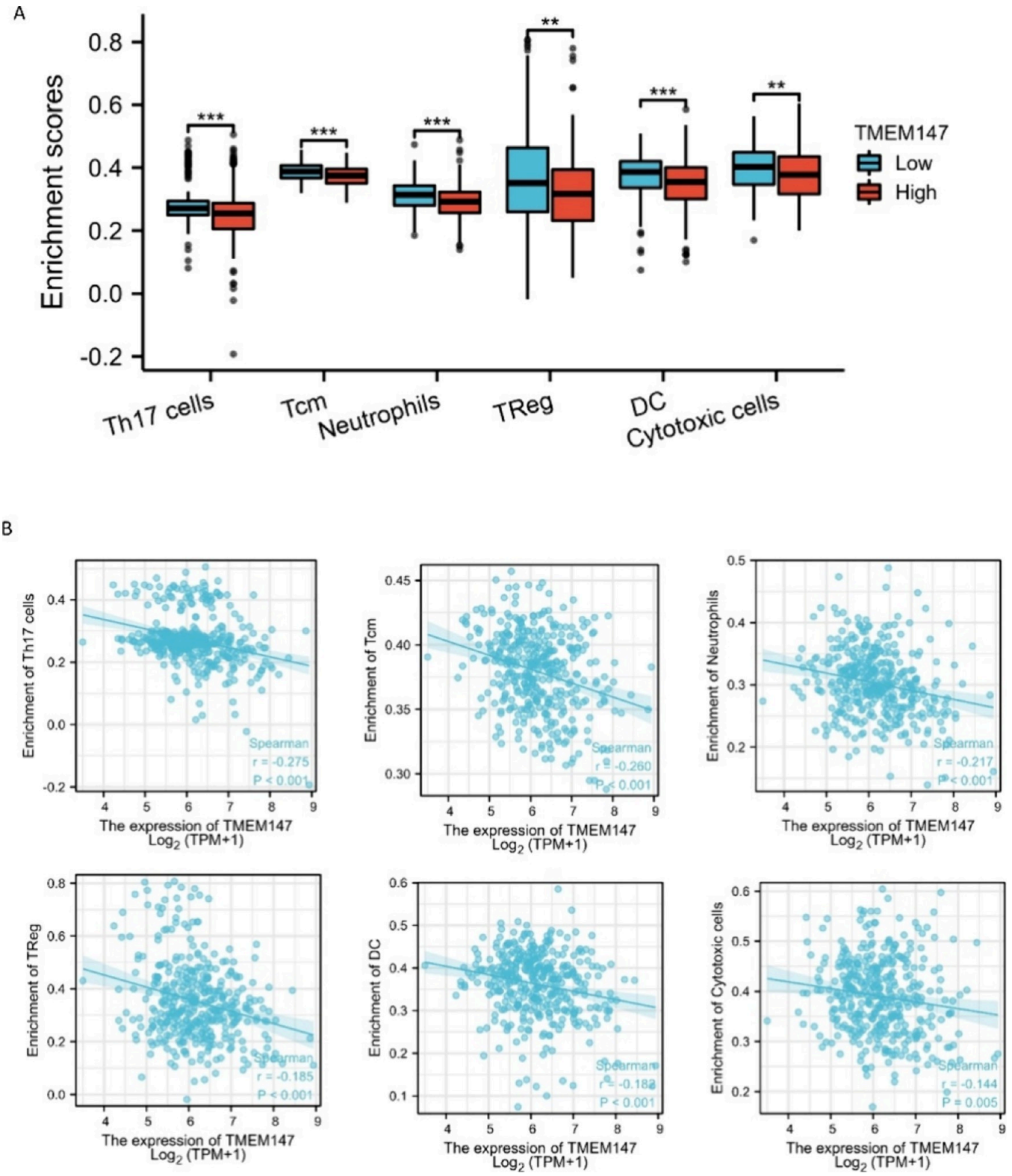

Figure 16. Analysis of the association of immune cell infiltration with TMEM147 expression in LIHC revealed 6 immune cell types that were positively related to TMEM147 expression. (A) Enrichment scores of TMEM147 expression in Th17 cells, Tcm cells, neutrophils, Tregs, DCs, and cytotoxic cells. (B) Correlation between TMEM147 expression and Th17 cells, Tcm cells, neutrophils, Tregs, DCs, and cytotoxic cells; ns, $P \geq 0.05$; *$P < 0.05$; **$P < 0.01$; ***$P < 0.001$.

proliferation, further confirming the clinical value of TMEM147 in the diagnosis of liver cancer.

In conclusion, this is the first study to investigate the oncogenic role of TMEM147 across cancers as well as its carcinogenic role in liver cancer. The identification of the diagnostic and prognostic significance of TMEM147 across cancers, and further exploration of its importance in LIHC, can provide new insights for the comprehensive understanding of

https://doi.org/10.1021/acsomega.4c01215
ACS Omega 2024, 9, 27137−27157

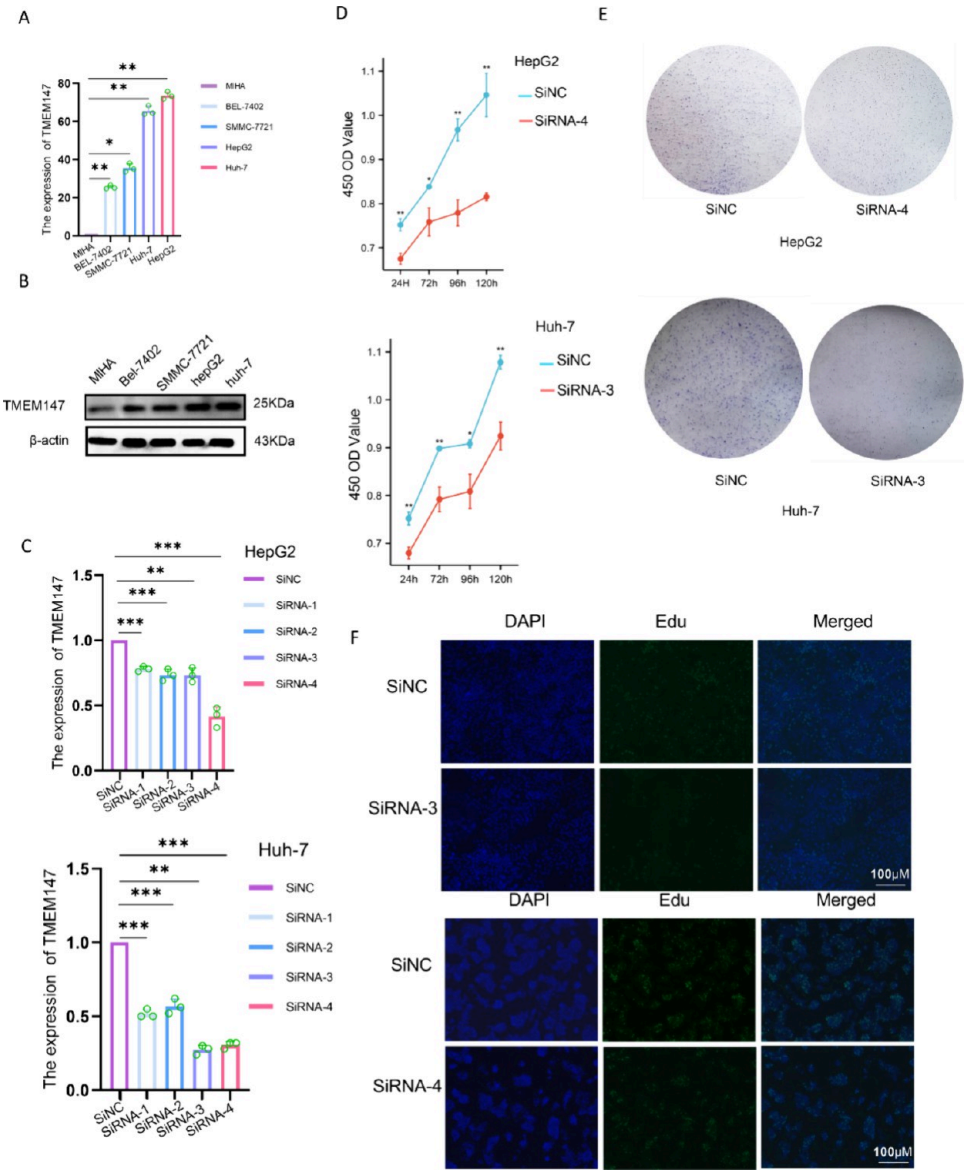

Figure 17. TMEM147 promoted cell proliferation in liver cancer. (A, B) TMEM147 is overexpressed in liver cancer cells. (C) siRNA was used to knock down TMEM147 expression in HepG2 and Huh-7 liver cancer cells. (D) The results of the CCK-8, (E) colony formation, and (F) EdU assays were obtained.

the key role of TMEM147 in tumor promotion and inhibition, provide a comprehensive basis for in-depth verification of its function in molecular biology experiments, and even provide integrated analysis results for the development of future cancer treatments for use in the clinic.

■ ASSOCIATED CONTENT

Data Availability Statement

The data sets generated during and/or analyzed during the current study are available in the Xiantao tool repository (https://www.xiantaozi.com) and TISIDB database (http://cis.hku.hk/TISIDB/index.php).

■ AUTHOR INFORMATION

Corresponding Author

Sumei Lu − *Department of Clinical Laboratory Medicine, The First Affiliated Hospital of Shandong First Medical University & Shandong Provincial Qianfoshan Hospital, Jinan 250000, China*; orcid.org/0000-0003-4969-0260; Phone: 18615218391; Email: lusumei@sdfmu.edu.cn

Authors

Yongqing Li − *Department of Clinical Laboratory Medicine, The First Affiliated Hospital of Shandong First Medical University & Shandong Provincial Qianfoshan Hospital, Jinan 250000, China*

Hanxiang Chen − *Department of Clinical Laboratory Medicine, The First Affiliated Hospital of Shandong First Medical University & Shandong Provincial Qianfoshan Hospital, Jinan 250000, China*

Bingyang Zhang − *Department of Clinical Laboratory Medicine, The First Affiliated Hospital of Shandong First Medical University & Shandong Provincial Qianfoshan Hospital, Jinan 250000, China*

Junjun Liu − *Department of Clinical Laboratory Medicine, The First Affiliated Hospital of Shandong First Medical University*

https://doi.org/10.1021/acsomega.4c01215
ACS Omega 2024, 9, 27137−27157

& Shandong Provincial Qianfoshan Hospital, Jinan 250000, China

Jianping Ma − *Department of Clinical Laboratory Medicine, The First Affiliated Hospital of Shandong First Medical University & Shandong Provincial Qianfoshan Hospital, Jinan 250000, China*

Wanshan Ma − *Department of Clinical Laboratory Medicine, The First Affiliated Hospital of Shandong First Medical University & Shandong Provincial Qianfoshan Hospital, Jinan 250000, China*

Complete contact information is available at: https://pubs.acs.org/10.1021/acsomega.4c01215

Notes

The authors declare no competing financial interest.

■ ACKNOWLEDGMENTS

This work was supported by the Natural Science Foundation of Shandong Province, China (grant nos. ZR2023MH031 and ZR2021MH187), Shandong First Medical University Youth Science Foundation Cultivation Support Program (grant no. 202201-083), and Cultivation Fund of National Natural Science Foundation of China in Shandong Provincial Qianfoshan Hospital (grant no. QYPY2021NSFC0804). Y.L. and S.L. conceived and designed the research, Y.L. acquired and analyzed the main data, H.C., B.Z., and J.L. helped in interpreting and analyzing the data, and W.M. analyzed and interpreted the data. All authors were involved in drafting and revising the manuscript.

■ REFERENCES

(1) Marx, S.; Dal Maso, T.; Chen, J. W.; Bury, M.; Wouters, J.; Michiels, C.; Le Calve, B. Transmembrane (TMEM) protein family members: Poorly characterized even if essential for the metastatic process. *Semin Cancer Biol.* **2020**, *60*, 96−106.

(2) Du, Y.; Zeng, X.; Yu, W.; Xie, W. A transmembrane protein family gene signature for overall survival prediction in osteosarcoma. *Front Genet* **2022**, *13*, No. 937300.

(3) Qiao, W.; Han, Y.; Jin, W.; Tian, M.; Chen, P.; Min, J.; Hu, H.; Xu, B.; Zhu, W.; Xiong, L.; Lin, Q. Overexpression and biological function of TMEM48 in non-small cell lung carcinoma. *Tumour Biol.* **2016**, *37* (2), 2575−86.

(4) Zhao, J.; Zhu, D.; Zhang, X.; Zhang, Y.; Zhou, J.; Dong, M. TMEM206 promotes the malignancy of colorectal cancer cells by interacting with AKT and extracellular signal-regulated kinase signaling pathways. *J. Cell Physiol* **2019**, *234* (7), 10888−10898.

(5) Cuajungco, M. P.; Podevin, W.; Valluri, V. K.; Bui, Q.; Nguyen, V. H.; Taylor, K. Abnormal accumulation of human transmembrane (TMEM)-176A and 176B proteins is associated with cancer pathology. *Acta Histochem* **2012**, *114* (7), 705−12.

(6) Thomas, Q.; Motta, M.; Gautier, T.; Zaki, M. S.; Ciolfi, A.; Paccaud, J.; Girodon, F.; Boespflug-Tanguy, O.; Besnard, T.; Kerkhof, J.; McConkey, H.; Masson, A.; Denomme-Pichon, A. S.; Cogne, B.; Trochu, E.; Vignard, V.; El It, F.; Rodan, L. H.; Alkhateeb, M. A.; Jamra, R. A.; Duplomb, L.; Tisserant, E.; Duffourd, Y.; Bruel, A. L.; Jackson, A.; Banka, S.; McEntagart, M.; Saggar, A.; Gleeson, J. G.; Sievert, D.; Bae, H.; Lee, B. H.; Kwon, K.; Seo, G. H.; Lee, H.; Saeed, A.; Anjum, N.; Cheema, H.; Alawbathani, S.; Khan, I.; Pinto-Basto, J.; Teoh, J.; Wong, J.; Sahari, U. B. M.; Houlden, H.; Zhelcheska, K.; Pannetier, M.; Awad, M. A.; Lesieur-Sebellin, M.; Barcia, G.; Amiel, J.; Delanne, J.; Philippe, C.; Faivre, L.; Odent, S.; Bertoli-Avella, A.; Thauvin, C.; Sadikovic, B.; Reversade, B.; Maroofian, R.; Govin, J.; Tartaglia, M.; Vitobello, A. Bi-allelic loss-of-function variants in TMEM147 cause moderate to profound intellectual disability with facial dysmorphism and pseudo-Pelger-Huet anomaly. *Am. J. Hum. Genet.* **2022**, *109* (10), 1909−1922.

(7) Dettmer, U.; Kuhn, P. H.; Abou-Ajram, C.; Lichtenthaler, S. F.; Kruger, M.; Kremmer, E.; Haass, C.; Haffner, C. Transmembrane protein 147 (TMEM147) is a novel component of the Nicalin-NOMO protein complex. *J. Biol. Chem.* **2010**, *285* (34), 26174−81.

(8) Lu, M.; Tian, X.; Yang, X.; Yuan, C.; Ehsan, M.; Liu, X.; Yan, R.; Xu, L.; Song, X.; Li, X. The N- and C-terminal carbohydrate recognition domains of Haemonchus contortus galectin bind to distinct receptors of goat PBMC and contribute differently to its immunomodulatory functions in host-parasite interactions. *Parasites Vectors* **2017**, *10* (1), 409.

(9) Christodoulou, A.; Maimaris, G.; Makrigiorgi, A.; Charidemou, E.; Luchtenborg, C.; Ververis, A.; Georgiou, R.; Lederer, C. W.; Haffner, C.; Brugger, B.; Santama, N. TMEM147 interacts with lamin B receptor, regulates its localization and levels, and affects cholesterol homeostasis. *J. Cell Sci.* **2020**, *133* (16), jcs245357 DOI: 10.1242/jcs.245357.

(10) Ota, M.; Tanaka, Y.; Nakagawa, I.; Jiang, J. J.; Arima, Y.; Kamimura, D.; Onodera, T.; Iwasaki, N.; Murakami, M. Role of Chondrocytes in the Development of Rheumatoid Arthritis Via Transmembrane Protein 147-Mediated NF-kappaB Activation. *Arthritis Rheumatol* **2020**, *72* (6), 931−942.

(11) Feng, Y.; Li, Y.; Li, L.; Wang, X.; Chen, Z. Identification of specific modules and significant genes associated with colon cancer by weighted gene co-expression network analysis. *Mol. Med. Rep.* **2019**, *20* (1), 693−700.

(12) Vivian, J.; Rao, A. A.; Nothaft, F. A.; Ketchum, C.; Armstrong, J.; Novak, A.; Pfeil, J.; Narkizian, J.; Deran, A. D.; Musselman-Brown, A.; Schmidt, H.; Amstutz, P.; Craft, B.; Goldman, M.; Rosenbloom, K.; Cline, M.; O'Connor, B.; Hanna, M.; Birger, C.; Kent, W. J.; Patterson, D. A.; Joseph, A. D.; Zhu, J.; Zaranek, S.; Getz, G.; Haussler, D.; Paten, B. Toil enables reproducible, open source, big biomedical data analyses. *Nat. Biotechnol.* **2017**, *35* (4), 314−316.

(13) Yu, G.; Wang, L. G.; Han, Y.; He, Q. Y. clusterProfiler: an R package for comparing biological themes among gene clusters. *OMICS* **2012**, *16* (5), 284−7.

(14) Liu, J.; Lichtenberg, T.; Hoadley, K. A.; Poisson, L. M.; Lazar, A. J.; Cherniack, A. D.; Kovatich, A. J.; Benz, C. C.; Levine, D. A.; Lee, A. V.; Omberg, L.; Wolf, D. M.; Shriver, C. D.; Thorsson, V.; The Cancer Genome Atlas Research Network; Hu, H. An Integrated TCGA Pan-Cancer Clinical Data Resource to Drive High-Quality Survival Outcome Analytics. *Cell* **2018**, *173* (2), 400−416.e11.

(15) Bindea, G.; Mlecnik, B.; Tosolini, M.; Kirilovsky, A.; Waldner, M.; Obenauf, A. C.; Angell, H.; Fredriksen, T.; Lafontaine, L.; Berger, A.; Bruneval, P.; Fridman, W. H.; Becker, C.; Pages, F.; Speicher, M. R.; Trajanoski, Z.; Galon, J. Spatiotemporal dynamics of intratumoral immune cells reveal the immune landscape in human cancer. *Immunity* **2013**, *39* (4), 782−95.

(16) Hanzelmann, S.; Castelo, R.; Guinney, J. GSVA: gene set variation analysis for microarray and RNA-Seq data. *BMC Bioinf.* **2013**, *14*, 7.

(17) Siegel, R. L.; Miller, K. D.; Fuchs, H. E.; Jemal, A. Cancer Statistics, 2021. *CA Cancer J. Clin* **2021**, *71* (1), 7−33.

(18) Zhang, N.; Pan, H.; Liang, X.; Xie, J.; Han, W. The roles of transmembrane family proteins in the regulation of store-operated Ca2+ entry. *Cell. Mol. Life Sci.* **2022**, *79* (2), 118.

(19) Jiang, X. Y.; Wang, L.; Liu, Z. Y.; Song, W. X.; Zhou, M.; Xi, L. TMEM48 promotes cell proliferation and invasion in cervical cancer via activation of the Wnt/beta-catenin pathway. *J. Recept Signal Transduct Res.* **2021**, *41* (4), 371−377.

(20) Zhang, S.; Dai, H.; Li, W.; Wang, R.; Wu, H.; Shen, M.; Hu, Y.; Xie, L.; Xing, Y. TMEM116 is required for lung cancer cell motility and metastasis through PDK1 signaling pathway. *Cell Death Dis* **2021**, *12* (12), 1086.

(21) Schmit, K.; Michiels, C. TMEM Proteins in Cancer: A Review. *Front. Pharmacol.* **2018**, *9*, 1345.

(22) Losic, B.; Craig, A. J.; Villacorta-Martin, C.; Martins-Filho, S. N.; Akers, N.; Chen, X.; Ahsen, M. E.; von Felden, J.; Labgaa, I.; D'Avola, D.; Allette, K.; Lira, S. A.; Furtado, G. C.; Garcia-Lezana, T.; Restrepo, P.; Stueck, A.; Ward, S. C.; Fiel, M. I.; Hiotis, S. P.; Gunasekaran, G.;

Sia, D.; Schadt, E. E.; Sebra, R.; Schwartz, M.; Llovet, J. M.; Thung, S.; Stolovitzky, G.; Villanueva, A. Intratumoral heterogeneity and clonal evolution in liver cancer. *Nat. Commun.* **2020**, *11* (1), 291.
(23) Calderaro, J.; Ziol, M.; Paradis, V.; Zucman-Rossi, J. Molecular and histological correlations in liver cancer. *J. Hepatol* **2019**, *71* (3), 616−630.
(24) Xiang, X.; Liu, Z.; Zhang, C.; Li, Z.; Gao, J.; Zhang, C.; Cao, Q.; Cheng, J.; Liu, H.; Chen, D.; Cheng, Q.; Zhang, N.; Xue, R.; Bai, F.; Zhu, J. IDH Mutation Subgroup Status Associates with Intratumor Heterogeneity and the Tumor Microenvironment in Intrahepatic Cholangiocarcinoma. *Adv. Sci.* **2021**, *8*, 2101230.
(25) Li, L.; Wang, H. Heterogeneity of liver cancer and personalized therapy. *Cancer Lett.* **2016**, *379* (2), 191−7.
(26) Villanueva, A. Hepatocellular Carcinoma. *N Engl J. Med.* **2019**, *380* (15), 1450−1462.
(27) Dongiovanni, P.; Romeo, S.; Valenti, L. Hepatocellular carcinoma in nonalcoholic fatty liver: role of environmental and genetic factors. *World J. Gastroenterol* **2014**, *20* (36), 12945−55.
(28) Brody, H.; Grayson, M.; Gravitz, L.; Miller, K.; Packwood, L. Liver cancer. *Nature* **2014**, *516* (7526), S1 DOI: 10.1038/516S1a.
(29) Vogel, A.; Meyer, T.; Sapisochin, G.; Salem, R.; Saborowski, A. Hepatocellular carcinoma. *Lancet* **2022**, *400* (10360), 1345−1362.
(30) Wang, Y.; Guo, Z.; Isah, A. D.; Chen, S.; Ren, Y.; Cai, H. Lipid metabolism and tumor immunotherapy. *Front. Cell Dev. Biol.* **2023**, *11*, 1187989.
(31) Sag, D.; Cekic, C.; Wu, R.; Linden, J.; Hedrick, C. C. The cholesterol transporter ABCG1 links cholesterol homeostasis and tumour immunity. *Nat. Commun.* **2015**, *6*, 6354.
(32) Satriano, L.; Lewinska, M.; Rodrigues, P. M.; Banales, J. M.; Andersen, J. B. Metabolic rearrangements in primary liver cancers: cause and consequences. *Nat. Rev. Gastroenterol Hepatol* **2019**, *16* (12), 748−766.
(33) Sun, H. W.; Yu, X. J.; Wu, W. C.; Chen, J.; Shi, M.; Zheng, L.; Xu, J. GLUT1 and ASCT2 as Predictors for Prognosis of Hepatocellular Carcinoma. *PLoS One* **2016**, *11* (12), No. e0168907.
(34) Jia, W.; Xie, G.; Jia, W. Bile acid−microbiota crosstalk in gastrointestinal inflammation and carcinogenesis. *Nature Reviews Gastroenterology & Hepatology* **2018**, *15* (2), 111−128.
(35) Nwosu, Z. C.; Megger, D. A.; Hammad, S.; Sitek, B.; Roessler, S.; Ebert, M. P.; Meyer, C.; Dooley, S. Identification of the Consistently Altered Metabolic Targets in Human Hepatocellular Caercinoma. *Cell Mol. Gastroenterol Hepatol* **2017**, *4* (2), 303−323e1.

https://doi.org/10.1021/acsomega.4c01215
ACS Omega 2024, 9, 27137−27157